ORF19.7060 and white-opaque switching in *MTL* a/α cells of *Candida albicans*

Masoumehzaman Alizadehnohi

A Thesis

in

The Department of Biology

Presented in Partial Fulfillment of the Requirements

for the Degree of

Master of Science (Biology) at

Concordia University

Montreal, Quebec, Canada

May

2020

CONCORDIA UNIVERSITY

School of Graduate Studies

This is to certify that the thesis prepared

By: Masoumehzaman Alizadehnohi

Entitled: *ORF19.7060* and white-opaque switching in *MTL* **a**/α cells of *Candida albicans*

and submitted in partial fulfillment of the requirements for the degree of

Master of Science (Biology)

complies with the regulations of the University and meets the accepted standards with respect to originality and quality.

Signed by the final Examining Committee:

Dr. Michael Sacher

_____ Chair

Dr. Patrick Gulick

_____ Examiner

Dr. Aashiq H. Kachroo

_____ Examiner

Dr. Malcolm Whiteway

_____ Supervisor

Dr. ROBERT WELADJI

Approved by _____

Chair of Department or Graduate Program Director

Summer *Dr. Andre G. Roy*

_____ 2020 _____

Dean of Faculty

Abstract

ORF19.7060 and white-opaque switching in *MTL* **a**/α cells of *Candida albicans*

Masoumeh Alizadeh, M.Sc.

Concordia University, 2020

Diploid *C. albicans* cells that are heterozygous for the *MTL* locus cannot mate, because they repress expression of the master regulatory protein Wor1 critical for activating the mating-competent opaque state. However, cells that lack or are heterozygous for sequences encompassing the shared promoter region of *ORFs 19.7061* and *19.7060* can switch to the opaque state even when heterozygous at *MTL*. Transcriptome analysis of *MTL* heterozygous strains where one (MA40) or both (MA10) alleles of 5'-UTR of *ORF19.7060* were deleted, shows that in spite of the formation of the a1-α2 repressor, the expression of *WOR1* occurred, allowing the cells to undergo white-opaque switching. Further investigation revealed that transcription factors such as *EFG1*, *RFG1* and specifically *SFL2* were down regulated in both MA10 and MA40 strains. However, these two strains cannot mate properly due to the **a**1-α2 repression of the mating genes. The ability of the *MTL* **a**/α cells to switch to the opaque state appears dependent on the size of the deletions; large deletions in the 5'-UTR of *ORF19.7060*, even in the heterozygous state, permit switching to classical opaque cells, smaller deletions in this region permit switching to an opaque-like state that exhibits opaque cell morphology but does not express a characteristic opaque-specific epitope on the cell surface, and even smaller deletions are not permissive for white to opaque switching. *ORF19.7060*, which encodes a protein with sequence similarity to enzymes implicated in non-homologous end joining, is one of the *C. albicans* genes that have different transcripts in white and opaque cells.

Acknowledgments

I would like to extend a sincere thanks to my supervisor Prof. Malcolm Whiteway for his guidance, informative feedback and encouragement throughout this process. The success of this project and my growth as a researcher were due in large part to his vast knowledge, patience, kindness, and support. I also want to thank my committee members, Prof. Patrick Gulick and Prof. Michael Sacher for their practical and useful advice and comments. Having the opportunity to work with such intelligent, passionate people was truly inspiring and was a great honor and chance for me.

In addition, I would like to thank the faculty and staff, and my friends Anna, Raha, Samira, Manjuri, Saima and Yana in the lab for their help and support, and colleagues in the Department of Biology, who made these years such a remarkable experience.

Finally, I would like to thank my family especially my sister Maryam and my brother in law Dimitry for their love and support.

Table of Contents

List of Figures

List of Tables

List of abbreviations

Calcofluor-white	CFW
Cyclic AMP- protein kinase A	cAMP-PKA
Clustered regularly interspaced short palindromic repeats	CRISPR
Gene replacement and conditional expression	GRACE
Luria-Bertani- Ampicillin	LB-AMP
Loss of heterozygosity	LOH
Mating type-like	*MTL*
N-Acetylglucosamine	GlcNAc
Non-Homologous-End-Joining	NHEJ
Nourseothricin	NAT
Phosphate-buffered saline	PBS
Polymerase chain reaction	PCR
Room temperature	RT
Scanning electronic microscope	SEM
Single guide RNA	sgRNA
Tetracycline	TET
Transcription Factors	TFs
Wild type	WT
White-to-Opaque switching	W/OP switching
Yeast extract, peptone, dextrose	YPD
Yeast Carbon Base- Bovine Serum Albumin	YCB-BSA

Introduction

1.1 *Candida albicans* and related pathogens

C. albicans is a diploid fungus with eight chromosome pairs in its genome and about 6,500 pairs of allelic genes[1]. *C. albicans* generally acts as a harmless, commensal yeast that can colonize different niches in the healthy human body such as the gastrointestinal tract, genital mucosa or oral mucosa without causing significant problems [2]. However, it can cause localized diseases, such as oral candidiasis and vaginitis [3], and the majority of females, at least once in their lifetime, will suffer from vaginal candidiasis[4]. Among the many Candida species, *C. albicans* also is a major cause of candidemia [5], and *C. albicans* systemic infections can generate mortality rates up to 40% in immunosuppressed people such as patients undergoing organ transplantation, receiving cancer chemotherapy, or infected with HIV [6, 7]. Even among survivors, the recurrence of the infection may happen anytime when the immune system is weakened, and patients frequently must be re-hospitalized [8].

1.2 Phenotypic plasticity

As a commensal organism, *C. albicans* has developed multiple strategies to adapt to living in the challenging conditions of a mammalian body. These include a variety of sophisticated signaling mechanisms which allow response to its external environments and facilitate proliferation and survival [9]. As an opportunistic pathogen, its success not only depends on its ability to sense environmental changes and adapt its physiology to its conditions, but also on its capability to grow in different morphological forms and transition among these forms[10]. This capacity is important for its survival within the physiological variation of the selected niches of the mammalian body. Among the morphologies exhibited by *C. albicans* are unicellular yeast forms defined as White, Opaque, Gut or Gray state cells [11], pseudo-hyphae, which are typically chains of elongated cells, elongated true hyphae, and biofilm forms that are mixtures of morphologies associated with an extracellular matrix [12, 13].

1.3 White vs Opaque

A specific phenotypic transition within unicellular yeast forms is termed white-opaque (W/OP) switching, and this transition has been identified as a prerequisite for mating in *C. albicans* [14].

W/OP switching was first identified in *C. albicans* in 1987, in strain WO-1, isolated from the blood and lungs of a clinical patient who suffered from a systemic infection [15]. The transition occurs between unicellular yeast forms, and is a spontaneous, stochastic, epigenetic and heritable event [16]. Opaque cells and white cells show differences in many characteristics, such as their active metabolic pathways [17], gene expression profiles [18], optimal temperature for growth [19], preferred niches in the host [20], acidic pH in their ambient niche [21], propensity for causing disease [11], cell morphology and colony shape When characterized for colony morphology on agar plates [22], white cells create shiny and dome-shaped colonies, while the opaque cells generate grayish, flatter colonies [15]. This difference becomes more distinct when Phloxine -B is added to the agar plate, in this case, opaque colonies stain pink due to differences in permeability of their cell wall, while the white cells form white dome-shaped colonies that do not stain or stain weakly (Fig.1.1)[23, 24].

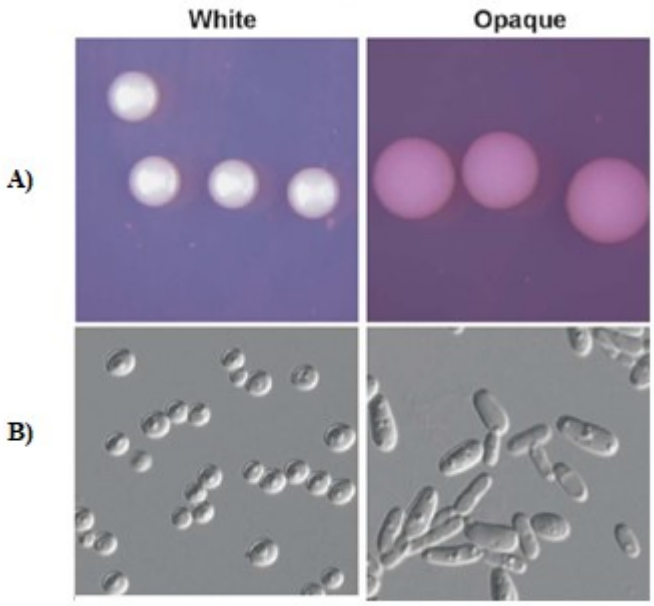

Figure 1.1 A) White colonies and opaque colonies on the plate. B) White and opaque cells. The morphological differences between white and opaque colonies and cells [25].

When observed under the microscope, white cells are oblate spheroids, while opaque cells are significantly larger and are elongated with a large vacuole (Fig.1.1) [26]. Transmission electron microscopic comparison of opaque cells and white cells showed opaque cells displayed a unique

cell surface that contains pimples [27]. As well, opaque cells express several different opaque-specific antigens on the cell surface [27]. In the human body, opaque cells occupy the skin and surface mucosal regions that are closer to their optimum temperature, which is 25˚C [28]. Studies demonstrated that changes in temperature from 25˚C to 30-37˚C drastically enhanced the transition of opaque cells to white state cells, which suggest that the white cells should be fitter in bloodstream infections than opaque cells [29].

Invasive infections involve Candida cells entering the blood stream and spreading through the body; this type of Candidemia mostly involves patients already suffering from conditions that suppress or weaken their immune system [30]. This type of infection is typically caused by white cells due to their optimal temperature fit to the specific host niche. By contrast, opaque cells are better at causing cutaneous infections and create less serious infections and are less virulent [31]. The less invasiveness of opaque cells compared to the white phase cells were shown in the studies that misexpression of *SAP1* (opaque specific gene) in white cells gives them the ability to utilize proteins as sole nitrogen source, and also enables them to occupy the skin by increasing adhesion [28]. The reduced invasiveness of opaque cells is not only because of the niches they occupy but also due to the fact that most conditions that induce white cells to be more invasive like the signals that can induce hyphal formation, do not affect opaque cells [32].

White cells can be selectively phagocytosed and killed by neutrophils in a mixed population of white and opaque cells, the opaque cells are not recognized by human polymorphonuclear neutrophils (PMNs) the resion behind this fact is opaque cells repress the genes that have a role in filamentation, therefore the PMNs can not recognized them as pathogen [20]. This selective recognition of PMNs can act in an environmentally dependent manner. The W/OP transition contributes to the various response to the host innate immune system and evasion toward *C. albicans* [20, 28, 33, 34]

The same environmental cues can activate different morphological transitions in *C. albicans*. In white **a**/α cells, GLcNAc activates cAMP-mediated signaling through the protein kinase A (PKA) complex, enhancing the expression of hypha-specific genes and triggering filamentation [35]. By contrast, in white a/a cells, when PKA is activated by GlcNAc or CO_2 it promotes W/OP switching rather than filamentation [36]. As well, a high throughput study examined white and opaque cells in almost 3000 different environmental conditions, and observed that white cells are more tolerant

toward environmental disruption, which makes them better at dealing with the different niches in the mammalian host [17].

These morphological and metabolic differences between white and opaque cells are consistent with gene expression profiles. Transcriptome analysis of the white and opaque established that about 400 genes are differentially regulated in white cells versus opaque cells, over 175 genes are up-regulated in white cells relative to opaque cells, while almost 240 genes are up-regulated in opaque cells relative to white cells [37, 38]. One of the key differences in gene expression represent genes involved in the mating process of *C. albicans* cells. These genes are uniquely expressed in opaque cells, and thus under normal conditions, only the opaque cells of *C. albicans* are mating competent [21].

1.4 Mating type genes in *Saccharomyces cerevisiae* vs *Candida albicans*:

C. albicans and *S. cerevisiae* are estimated to have split from their common ancestor sometime between 100 to 800 million years ago [39], and these two organisms share many similarities as well as differences. Their sex determination circuitry is one of their major similarities. Although each organism has unique characteristics, the overall structure of the cell-type determination and mating signalling pathways are fundamentally similar. In *S. cerevisiae,* the cell type determination circuit was worked out in the 1970 – 1980s [40]. The mating type is determined by two distinct non-homologous alleles at the *MAT* (mating type) locus. *MAT**a*** encodes the a1 gene and defines the mating type a phenotype; *MATα* encodes the *MATα1* and *MATα2* genes and defines the alpha mating type phenotype. The "**a**" phenotype is the default phenotype in *S. cerevisiae*; deletion of the entire *MAT* locus creates a phenotypically *MAT**a*** cell termed an Alf for "**a**-like faker" [41]. Consequently, the **a**1 protein has no function in *MAT***a** cells but plays a key role in diploid cells [42]. The *MATα1* and *MATα2* gene products of the *MAT*α locus have distinct functions. The alpha1 protein is an activator that turns on the α-specific genes required for defining the α-specific mating functions. The alpha 2 protein serves as a repressor of the otherwise constitutive **a**-specific genes that define the **a**-mating functions (Fig.1.4.1). Conjugation between these two mating type cells leads to non-mating **a**/α diploid cells. These diploid cells are non-mating because the combination of the **a**1 protein and the alpha 2 protein creates a repressor (**a**1-α2) that shuts off the α-specific genes by suppressing the alpha 1 activator, while alpha 2 continues to supress the **a**-specific genes [42].

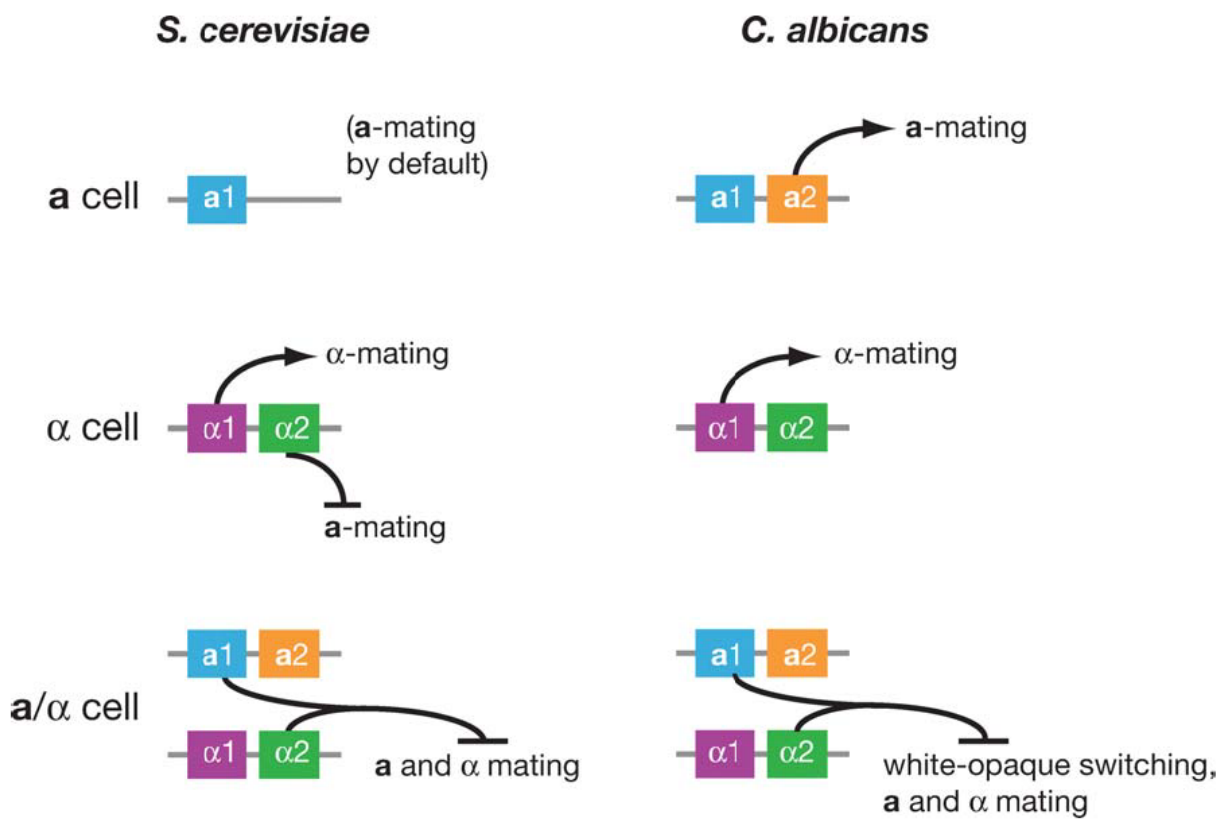

Figure 1.2 *S. cerevisiae MAT**a*** and *MATalpha* loci compared with *MTL**a*** and *MTLalpha* loci in *C. albicans* [26].

C. *albicans* as an obligate diploid yeast [26], and was thought to be asexual and non-mating until 1999, when genome sequencing studies identified a mating type like (*MTL*) locus with elements of similarity to the *MAT* locus of *S. cerevisiae*. In addition to non-mating related genes for an oxysterol binding protein (*OBP*), a PI kinase (*PIK*) and a polyA binding protein (*PAP*), this locus contained orthologs of *MAT**a**1* (*MTL***a***1*), *MATalpha1* (*MTLalpha1*) and *MATalpha2* (*MTLalpha*2) [24, 43], and was later seen to contain a unique *MTL***a***2* gene (Fig.1.2) [44]. In the following years this observation opened the study of the mating response pathway in *C. albicans* [38]. In *C. albicans* strains where *MTL* heterozygosity was lost by deletions of *MTL* **a** or *MTLalpha* information (34), or by homozygosis of the locus to *MTL* **a**/**a** or *MTL* α/α [45] cells were mating competent, while *MTL* **a**/*α* stain are non-mating [17]. The discovery of *MTL**a**2* in *C. albicans* suggested a positive regulation circuit for the **a**-type pathway functioned in a common ancestor,

and this circuit, during evolution, has presumably been lost in *S. cerevisiae,* or perhaps lost in an ancestor and regained by *C. albicans* [30]. However, although the *MTL* homozygous strains could mate, their mating efficiency was dramatically lower than that of *S. cerevisiae* [24, 46].

Although the architectures of the *MAT* and *MTL* loci are quite similar, the circuits have fundamental differences [47]. In *C. albicans*, the circuits are controlled positively. Cells homozygous for *MTL* **a** function are **a** maters because they express *MTLa2*, which is a positive regulator of **a**-specific functions required for mating, while cells homozygous for *MTLalpha* function are α maters because they express *MTLalpha1* which is a positive regulator of the α-specific functions required for mating. Cells which are heterozygous (**a**/α) at *MTL* are non-mating because they express a repressor (**a**1-α2) which shuts off **a** and α -specific functions by suppressing these *MTL**a**2* and *MTLalpha1* positive regulators [26]. In *S. cerevisiae* the cell type establishment circuits also involve negative control. Haploid **a**-type cells express the haploid-specific **a**-genes constitutively, and thus loss of the *MAT* locus leads to **a**-specific mating. Haploid α-type cells express the α-type-specific genes under control of *MATalpha1* as in *C. albicans* but eliminate **a**-specific gene expression with the repressor *MATalpha2*. Thus in *S. cerevisiae* **a**-specific genes need to be repressed when not needed, while in *C. albicans* they are just not expressed without the activator *MTL**a**2* [47]. In both organisms, cells of opposite mating types can mate and become heterozygous at the mating type control loci *MAT* or *MTL*. In *S. cerevisiae* this heterozygous cell is typically diploid, is non-mating and can undergo meiosis and sporulation [33]. In *C. albicans*, on the other hand, the standard cell is the heterozygous **a**/α diploid, and the typical mating arrangement generates a tetraploid cell. There is no evidence for meiosis and sporulation in these tetraploid cells [26, 48], or in the *MTL* **a**/α diploids. Rare haploid *C. albicans* cells have been identified, but they are very unstable and revert to the diploid state easily [49]. In general, the tetraploid **aa**/αα cells reduce ploidy and regenerate three different cell types, diploid **a**/**a**, α/α, and **a**/α cells through a "parasexual" process of cell division and chromosome loss [46].

As well as the differences in the logic of the cell type determining circuitry and the mechanisms of completing the mating cycle, *C. albicans* and *S. cerevisiae* have a major difference in the determination of the mating competent state. *S. cerevisiae* cells that are homozygous for the *MAT* locus, as either the typical haploid or as **a/a** or α/α diploids, are intrinsically mating competent. By contrast, *MTL* homozygous *C. albicans* cells are not inherently mating competent, they first have to switch from their regular yeast form to the elongated and larger opaque state cell [50]. This

transition is controlled by layers of interlocking transcriptional regulation but is epigenetic [51] and is fundamentally driven by the activation of an auto-regulated transcription factor termed Wor1[52]. Only these opaque cells are mating competent [51, 53, 54].

Thus in nature, for *C. albicans* to become mating competent, cells must first undergo the rare event of loss of *MTL* heterozygosity [55], then these standard white cell *MTL* homozygotes (**a**/**a** or α/α), must transient to the mating competent opaque state, which is another rare event. This second step is also inhibited at 37˚C, which is the typical temperature of the human host [56]. Even if *C. albicans* cells do enter the mating competent opaque state, they still need to come in contact with a mating competent partner of the opposite mating type cell type to undergo conjugation. This suggests mating will be an infrequent event in nature, and studies on natural populations show little evidence for extensive genetic interchange driven by conjugation [57].

1.5 The *MTL* locus controls the white-opaque transition in *Candida albicans*:

The **a**1-α2 heteromeric repressor acts in *S. cerevisiae* to block mating and to permit meiosis and sporulation by supressing the repressor of meiosis Rme1 [33]. The equivalent **a**1-a2 repressor in *C. albicans* acts to repress the white-opaque transition. This ensures that the typical *MTL* heterozygous diploid cell is unable to enter the mating competent opaque state, both because **a**1-α2 suppresses the positive regulators *MTL**a**2* and *MTLalpha1*, thus blocking **a** and α-specific gene expression, and because it also represses *WOR1*, the opaque circuitry master regulator. Once the **a**1-α2 repressor is removed through either the spontaneous formation of *MTL* **a/a** or *MTLα/α* forms in nature, or their induction in the lab through genetic engineering [45] or growing strains on sorbose and selecting the homozygous strain due to loss of one copy of chromosome 5 [58], the cells have the potential to become opaque.

In *MTL* homozygous cells the establishment of the opaque phenotype depends on the induction of a positive feedback loop for the autoregulated Wor1 transcriptional activator. *WOR1* positively regulates W/OP switching in an all-or-none pattern [53] and establishes the opaque phase circuit by up-regulating itself, as well as downstream transcriptional regulators such as *WOR2*, *WOR3* and *CZF1,* and by down-regulating *AHR1* and *EFG1*, a key negative regulator of opaque formation [14]. In 2016, *WOR4* was identified as a new transcriptional regulator that plays an indeterminate role inside this interlocking network but seems to function upstream of *WOR1*. Although ectopic expression of *WOR4* caused massive switching to the opaque state, and deletion of this gene

blocked the cell in a white state, this switching is blocked in a *WOR1* null deletion, suggesting the transition still depends on the *WOR1* expression. However, the expression of *WOR4* does not show drastic differences between white and opaque state cells [59]. These transcriptional regulators mentioned above control the opaque specific genes as well as mating specific genes. Thus the opaque circuit initiation is not yet fully understood, but the up-regulation of *WOR1* can be considered the key regulator of this process [60].

Although **a**1-α2 is considered to be the main repressor of the W/OP switching circuitry, *EFG1* as a white specific transcription factor plays a key role in maintaining the white state in the cells in *MTL* **a**/*α* genotype, and a recent study suggested that half of W/OP transitions in clinically isolated strains happened due to mutations in *EFG1* [61]. It has also been reported that individual deletion of some transcriptional regulators such as *RFG1, BRG1* and *SFL2* de-repress W/OP switching in *MTL* **a**/*α* cells [62]. As well, deletion of *OFR1*, which encodes an Yci domain protein, allows W/OP switching and mating in *MTL* **a**/α heterozygotes [62].

My study investigates the de-repression of the W/OP transition in *MTL* **a**/*α* cells caused by deletions in the *ORF19.7061/ORF19.7060* region. Previous studies on the GRACE Version 1.0 library to find genes that have a role in the W/OP transition in *MTL* **a**/*α* strains showed deletion of *ORF19.7061* is permissive to W/OP switching in cells are heterozygous at the *MTL* locus. However, deletions which removed the coding regions of either *ORF19.7060* or *ORF19.7061* could not be complemented for the permissive white-opaque switching phenotype by expressing either *ORF* driven by *ACT1* promoter at the *RP10* locus. The expression of these genes driven by the *ACT1* promter showed levels even more than the indigenous promoters, suggesting the failure to complement the phenotypes was not due to expression issues. Thus the switching phenotype may result from the disruption of the overall structure of the region, and not simply inactivation of the coding regions. This could result from bypassing the usual inhibition of mating-type like locus caused by white-specific transcriptional regulators such as *EFG1*, *RFG1* and specifically *SFL2*. I also found different phenotypes were created by different sized deletions of this region. Perhaps surprisingly, deletions in the 5'-UTR of *ORF19.7060* generated their phenotype as heterozygotes. These characteristics of a phenotypic dependence of the size of the deletion of the non-coding region, together with the ability of the mutations to function as heterozygotes, makes the connection between the *ORF19.7061/ORF19.7060* region and white-opaque switching an intriguing topic for study.

2.Materials and methods

2.1 Strains, Media and Culture conditions

The strains used or created in this experiment are shown in Table 1.

The "solo system" protocol of *C. albicans* CRISPR-Cas9 [63] was used for creating mutant strains; this protocol has the advantage of being able to generate homozygous mutations in one step. We designed three sets of primers for each CRISPR mutant construction: the sgRNA, repair DNA, and screening primers. The list of primers is shown in Table S1.

To design the sgRNAs, Benchling was used based on the guidelines as follows; single guide; Guide length: 20; Genome: CA22 (CANDIDA ALBICANS SC5314 (DILOID)); PAM: NGG. A guide sequence was chosen based on the position nearer to the stop codon (for gene replacement) and higher on-target and lower off-target scores. The candidate sequence was also checked in a file named (Targ.NoTs. subs12nt.HitsGenesOnly, Hits1 Gene2Alle. 3letterName) from the supplemental material of Vyas, et al 2015. This file shows sequences that provide a target in both alleles for any given gene. For the solo system the pV1093 plasmid with *CAS9* has *Amp* as a marker to use in *E. coli* transformation. The sgRNA (20 nt) has extended sequences that represent the complementary sequences on both 5' and 3' ends to allow cloning into the *BsmB*I site of plasmid PV1093. Therefore, this set of primers had the structure: Forward – 5'-atttgX20g-3' and Reverse – 5'-aaaacX20c-3'. The repair DNA was also designed through Benchling, *ORF19.7060/ORF19.7060* and the sgRNA were amplified using PCR from relevant plasmids and used for the CRISPR transient mutant construction [64]. The transient CRISPR protocol avoids *CAS9* being integrated into the *Candida* genome. The marker *HIS1* was amplified by PCR from plasmid pFA-CaHIS1 and primers provided enough homology to the flanking regions of *ORF19.7060/ORF19.7060*. The *HIS1* marker was transformed into the parental strain SN76 [9], and the transformants were selected on SD-his$^-$ agar plates. Successful transformants were further confirmed by colony PCR.

Heterozygous deletions of the the 5'-UTR of *ORF19.7060* were created by one-step traditional disruption [65, 66]. The *HIS1* marker with suitable flanking sequences was used as the selectable marker to direct replacement-insertion into the the 5'-UTR of *ORF19.7060* of one allele in strain SN76. Different 3' flanking sequences were used to create a nested series of deletions. Homozygous deletion of the the 5'-UTR of *ORF19.7060* was performed by the CRISPR-Cas9

method for *C. albicans* using a repair template of *HIS1* with suitable flanking sequences to direct the replacement insertion into both chromosomal alleles of SN76.

Strain	Parent	Mating type	Description	Source
SN76	RM1000	**a**/α	*arg4/arg4; his1/his1*; *ura3*:: imm434/*ura3*:: imm434	Noble/ Johnson
MA10	SN76	**a**/α	*arg4/arg4; ura3* ::imm434/*ura3* ::imm434; *ORF19.7061*+ *ORF19.7060* the 5'-UTR of *ORF19.7060* Δ/Δ	This study
MA20	SN76	**a**/α	*arg4/arg4; ura3*:: imm434/*ura3*:: imm434 *ORF19.7060* Δ/Δ	This study
MA30	SN76	**a**/α	*arg4/arg4; ura3*:: imm434/*ura3* ::imm434 *ORF19.7060* Δ/+	This study
MA40	SN76	**a**/α	*arg4/arg4; ura3*:: imm434/*ura3*:: imm434 *ORF19.7061*+*ORF19.7060* the 5'-UTR of *ORF19.7060* Δ/+	This study
MA110	MA10	**a**/α	*arg4/arg4 ORF19.7061*+ *ORF19.7060* the 5'-UTR of *ORF19.7060* Δ/Δ CIP *ORF19.7061*	This study
MA201	SN76	**a**/α	*arg4/arg4; ura3*:: imm434/*ura3*:: imm434 *ORF19.7060* the 5'-UTR of *ORF19.7060* Δ/+(860 nt)	This study
MA202	SN76	**a**/α	*arg4/arg4; ura3*:: imm434/*ura3* ::imm434 *ORF19.7060* the 5'-UTR of *ORF19.7060* Δ/+ (706 nt)	This study
MA203	SN76	**a**/α	*arg4/arg4; ura3* ::imm434/*ura3*:: imm434 *ORF19.7060* the 5'-UTR of *ORF19.7060* Δ/+ (625 nt)	This study
MA204	SN76	**a**/α	*arg4/arg4; ura3::* imm434/*ura3::* imm434 *ORF19.7060* the 5'-UTR of *ORF19.7060* Δ/+ (552 nt)	This study
MA205	SN76	**a**/α	*arg4/arg4; ura3*:: imm434/*ura3*:: imm434 *ORF19.7060* the 5'-UTR of *ORF19.7060* Δ/+ (475 nt)	This study
MA206	SN76	**a**/α	*arg4/arg4; ura3*:: imm434/*ura3* ::imm434 *ORF19.7060* the 5'-UTR of *ORF19.7060* Δ/+ (398 nt)	This study

MA207	SN76	**a**/α	*arg4/arg4; ura3::* imm434/*ura3* ::imm434 *ORF19.7060 the* 5'-UTR of *ORF19.7060* Δ/+ (321 nt)	This study
MA208	SN76	**a**/α	*arg4/arg4; ura3::* imm434/*ura3* ::imm434 *ORF19.7060 The* 5'-UTR of *ORF19.7060* Δ/+ (208 nt)	This study
CAI-4 *MTL* **a/a**	CAI-4	**a/a**	*ura3*:: imm434/ *ura3* ::imm434	Doreen Harcus
CAI-4 *MTL* α /α	CAI-4	α /α	*ura3*:: imm434/ *ura3* ::imm434	Doreen Harcus
3745	A505	**a/a**	*trp1/trp1; lys2/lys2*	Magee
3315	A505	α /α	*trp1/trp1; lys2/lys2*	Magee

Table 2.1 Strains used and created in this study. The symbol Δ/+ represents a heterozygous deletion in the region noted and the symbol Δ/Δ represents a homozygous deletion at the region.

2.1.1. Complementation:

Complementation of *MA10* to potentially reverse the W/OP switching phenotype was performed in three sequential steps. At first, PCR products consisting of *ORF19.6071*, *ORF19.7060* long transcript, *ORF19.7060* short transcript, and both *ORF19.7061* and *ORF19.6070* were constructed. Secondly, all the PCR constructs were ligated into plasmid CIP10 [67]. to place them under control of the *ACT1* promoter and transformed them into *E. coli* for amplification. Finally, the positively transformed plasmids were sequenced to confirm the accuracy of the constructs and linearized by *Stu*I at the RPS10 site and transformed into strains MA20(*ORF19.7060Δ/Δ),* MA10 (*ORF19.7060Δ/Δ* promoter deletion), MA40 (*ORF19.7060Δ/+*promoter deletion*), MA30 (ORF19.7060 Δ/+)* SN76 (WT), and CAI4. The transformants were selected on SD-ura^{-} agar plates. The successful transformants were further confirmed by colony PCR. Primers used in this study are listed in Table S1.

It is necessary to add that for general growth and maintenance of the strains in the white phase, the cells were cultured in fresh YPD medium (1% yeast extract, 2% Bacto peptone, 2% dextrose, 2% agar for solid medium, PH 6.5) at 30°C. In addition, two synthetic complete mediums were used as the strain switching indicators to monitor white phase colonies and opaque phase colonies in

three rounds of screening. The initial synthetic complete medium had N-acetylglucosamine (GlcNAc) as carbon source; (0.67% yeast nitrogen base, 0.15% amino acid mix with uridine at 100 µg/ml, 1.25% GlcNAc, and 2% agar for solid medium) [18]. The next synthetic complete medium was with dextrose as a carbon source (SD; 0.67% yeast nitrogen base, 0.15% amino acid mix with uridine at 100 µg/ml, 2% dextrose, and 2% agar for solid medium). Phloxine-B (5µg ml-1) was also added to nutrient agar for opaque colony staining [68]. The screening for W/OP switching over the mentioned cultures SD medium was done at
room temperature, this temperature was critical for maintaining the cells in the opaque phase.

2.1.2. Plasmid constructs and *Escherichia coli* transformation

The architecture of the CIP plasmid is shown in Figure3.4. The plasmid contains an ampicillin resistance gene to permit selection in *E. coli* and the *URA3* marker for selection in *C. albicans*. In addition, the plasmid contains a poly-linker which is located after the *ACT1* promoter. This polylinker lets us insert the PCR product under the control of this promoter. Amplifying primers were designed to contain *Xma*I and *Hind*III restriction sites to allow directional insertion into the polylinker site. The PCR constructs were amplified from the genomic DNA of WT strain SN148. The plasmid (CIP) and PCR products were both digested with *Xma*I and *Hind*III for four hours at 37˚C. Then both enzymes were heat-inactivated at 80˚C for 20 minutes prior to ligation. Subsequently, both PCR products and plasmids were ligated overnight at 16˚C to improve the efficiency of the ligation. The next day, DNA ligase was inactivated at 65˚C for 10 minutes and the ligated plasmid and PCR product was transformed into *E. coli* competent cells. In order to transform the plasmid into DH5α, (the *E. coli* strain) both *E. coli* and DNA were incubated on ice for 30 minutes and then samples were put into the water bath for heat shock at 42˚C for 90 seconds. Subsequently, the samples were put back on the ice for another 5 minutes and finally LB media without AMP was added to samples in order to let the cells to express the antibiotic resistance gene.

Afterward, the samples were plated on LB-AMP on 37˚C to grow. On the following day, the transformed colonies from the LB-AMP plate were selected, and plasmids were extracted and sequenced to confirm the correct insertion of the PCR products. Then confirmed plasmids were linearized and transformed into *C. albicans*.

Since the plasmid contains *URA3* for selection during the transformation process on *C. albicans* the transformed candidate was selected on SD-ura^{-} agar plates to identify transformants, and positive transformants were further confirmed by colony PCR.

2.2 Phenotype switching

To analyze and assess the ability of W/OP switching in the mutant strains, the transformed strains were streaked over the SC-GlcNAc media for a duration of 5 days at 25°C. In order to measure the ratio of W/OP transition in mutant strains, a single colony with white and opaque traits were picked up and suspended in SC- GlcNAc liquid medium to allow the cells to grow for overnight at room temperature with 220 rpm shaking. The next day, the cells concentration was adjusted to OD_{600}:1.0, and the suitable concentrations were plated on agar media containing 5 µg ml^{-1} phloxine-B with either 2% glucose or 1.25% GlcNAc as a carbon source. The mentioned plates were incubated at 25°C for a duration of 5 to 7 days. They were scanned on the 7th day and the frequency of pink colonies was calculated by standard statistical methods. The frequency of switching colonies was calculated by dividing the number of opaque colonies over the total number of colonies for white to opaque switching.

2.3 Microscopy and imaging

To confirm the identity of true opaque cells in the mutant strains, optical microscopic images of cells were captured using a Nikon Eclipse TS100. Immunofluorescence microscopic images were visualized and photographed using LeicaDS6000 with 630x magnification with settings: Objective: 63x Oil, Filter: TxRed-560/40. Images of plates and colonies were scanned at 800pi by an Epson Perfection v500 photo scanner.

2.3.1. Immunofluorescence staining microscopy

The true opaque cells produce specific antigens on their cell surface that can be recognized by the opaque specific antibody. This antibody can be conjugated with the secondary antibody which will be illustrated by Immunofluorescence microscopic imaging.

To perform the Immunofluorescence staining, the opaque or white colonies from individual plates were cultured overnight on SC-media at RT, 220rpm shaking and then diluted in fresh SD liquid media for another 12-hours incubation at RT, 220rpm. The cells were pelleted and washed in 1 ml

of 1xPBS three times, each time for 2 minutes. Approximately, 10^7 cells were tested for each further staining assay. The washed cells were blocked with a 1ml blocking buffer for 30 minutes before incubation with 100µl of the primary antibody for one hour at RT. Subsequently, the cells which were treated with primary antibody were washed once more with PBS containing 0.05%Tween 20 for three times, for 5 minutes each time. Washed cells were incubated with 100µl of the secondary antibody- Texas red conjugated goat anti-mouse antibody (1/100 dilution in blocking buffer) for 1 hour in the dark at RT. The cells were washed with PBS containing 0.05%Tween 20 three times and PBS once, for 5 min each time. Cells were finally suspended in 50µl PBS, and 3µl was applied under a coverslip. Sampled microscope slides were sealed and placed in a microscope slide box for protection from light before observation under the Leica DM6000 fluorescence microscope.

2.4 Mating assays

Knowing that W/OP switching is the prerequisite process for mating in *C. albicans* [12], the mating competency of all experimental strains were tested. First, all the assayed strains were maintained in the opaque phase at room temperature. Experimental and tester strains were streaked as straight lines on separate SC-GLcNAc and YPD plates. After 24-48 hours of incubation at room temperature, the two sets of streaks were cross-printed onto a single fresh SC-GLcNAc plate and YPD plate and incubated for another 24-48 hours at room temperature. At the end of this incubation, cells were replicated to drop-out plates containing SD medium minus two supplements (Uridine and Tryptophan) for selection of mating products, and to YPD plates as a control. All the plates were incubated at 30˚C for 2 days and scanned. Colonies appearing after 2 days demonstrated that mating identified through auxotrophic marker complementation had occurred with strain 3315 as the *MTL*α/α tester strain and 3745 as *MTL* **a/a** tester strain[69] .

2.5 RNA-Sequencing

RNA was extracted from strains SN76 (WT control), MA10 *(ORF19.7061 and the* 5'-UTR of *ORF19.7060* between two genes*)* and MA40 *(ORF19.7060/ORF19.7060Δ/+*promoter region*)* growing in the opaque phase, treatment following the QIAGEN RNA extraction kit protocol except the cells were disrupted completely with bead beater shaking for 25 times for 20 seconds and 1 minute for the cooling interval. Samples were tested for quality control by using a

bioanalyzer and submitted to the Genome Quebec Innovation Center for the construction of sequencing libraries. Subsequently, constructed libraries utilized for sequencing by using an Illumina Miseq. The results were scrutinized for finding the genes which were involved in the opaque pathway.

2.6 Western blotting

Western blotting was chosen to study the Orf19.7060 protein. This protein contains an XLF domain. This method allows us to inspect the difference between the mobility of the Orf19.7060 protein in white and opaque cells. *Orf19.7060* was TAP tagged, and both white and opaque cells of two independently tagged strains were grown in SD-GlcNAc liquid media for 24 hours at RT. Cells were then harvested by centrifugation, washed with distilled water and frozen at -80˚C for 24 hours, then freeze-dried in a lyophilizer for another 24 hours. The dried cells were then lysed by grinding in HK buffer supplemented with a protease inhibitor cocktail. The protein extract was clarified by centrifugation at 13000 rpm at 4˚C for one hour and the protein concentration measured by Bradford's Method [70] and equal amounts of proteins were suspended in SDS gel loading buffer, boiled and then resolved on 4–20% gradient SDS polyacrylamide gels. The separated polypeptides were transferred by electrophoresis onto a nitrocellulose membrane and analyzed by Western blotting using an anti–TAP polyclonal antibody [71]. The membrane was developed using the Li-Cor Odyssey system using their anti-rabbit-IR-Dye 680-conjugated secondary antibody [72].

2.7 Phenotypic assay for complementation of *ORF19.7060* strains:

To confirm complementation, a phenotypic assay was performed to assess the functionality of the *ORF19.7061* clone expressed from the *ACT1* promoter in strain MA10. From the original GRACE version 1.0 library, *ORF19.7061* was deleted, permitting the W/OP transition in the a/α strain. Further investigations provided more evidence that the adjacent gene *ORF19.7060* is responsible for the opaque transition in this mutant strain. In order to test this idea, I complemented the *ORF19.7061* mutant strain.

The PCR product of *ORF19.7061* was expressed under the *ACT1* promoter in the plasmid CIP. Strain *MA10* (derived from background strain SN76) was transformed with a linearized plasmid

containing an *ORF19.7060* PCR product under the *ACT1* promoter. To test successful complementation, I designed three different experiments as previously described.

Based on Saccharomyces GENOME DATABASE, *ORF19.7061* is an ortholog for *YHF7*, which encodes a putative uridine kinase. GENOME DATABASE suggested that this gene in Candida may have the same null phenotypes of CFW sensitivity. Then successful transformants of *ORF19.7061* PCR construct under *ACT1* promoter gain the sensitivity to Calcofluor white (CFW) in different concentrations. In addition, the phenotypic experiment was repeated for Congo red for further confirmation. The result of phenotypic assay demonstrated that the function of *ORF19.7061* has been complemented but the W/OP switching was not blocked.

2.8 Secreted aspartyl proteinase (SAP) activity

Transformants confirmed by colony PCR were selected, and a single colony was inoculated overnight in liquid YPD. The next day, cells adjusted to OD_{600}:1.0 were taken and from each sample 5 µl spotted on YCB-BSA plate and kept in 30˚C for 7 days [25] The halo around the spots was measured and the average of halo size determined.

Results

3.1 Identification of GRACE version 1.0 strain permissive for white-opaque switching in *MTL a/α* background

Normal *MTL* **a**/α cells are unable to undergo a switch from the white form to the opaque form, a process termed the white to opaque (W/OP) transition [38]. Screening of the GRACE version 1.0 library of inactivated *C. albicans* genes [73] for genes regulating the W/OP transition identified perturbation of *ORF19.7061* as permissive for W/OP switching in a *MTL* **a**/*α* background. However, in this region, the close proximity of genes *ORF19.7061* and *ORF19.7060* means that modifications to one gene typically will impact both genes. The close proximity of the genes raises a question of promoter structure; in the case of *ORF19.7060* and *ORF19.7061* expression is divergent and regulated by different promoters. (Fig.3.1 A). In the GRACE Version 1.0 library strain 47H7 the *HIS* replacement of one allele of *ORF19.7061* also deleted a white-specific promoter for the adjacent gene, *ORF19.7060*, while the *TET*-regulated promoter replacement of the other allele removed an opaque-specific promoter and more than 70 amino acids from the start of *ORF19.7060* (Fig.3.1B). Similarly, a deletion of the open reading frame of *ORF19.7060* would remove the transcription start site of *ORF19.7061*. Considering that *ORF19.7060* is one of the genes expressing different sized transcripts in white and opaque cells, it was possible that the impact on W/OP switching of the structural changes in strain 47H7 was caused by disrupting the normal expression of *ORF19.7060*, or the 5'-UTR of *ORF19.7060* rather than disrupting the structural region of *ORF19.7061*. I decided to investigate this genomic region in more detail to establish the genetic determinants at this locus controlling W/OP switching in *MTL* **a**/α cells.

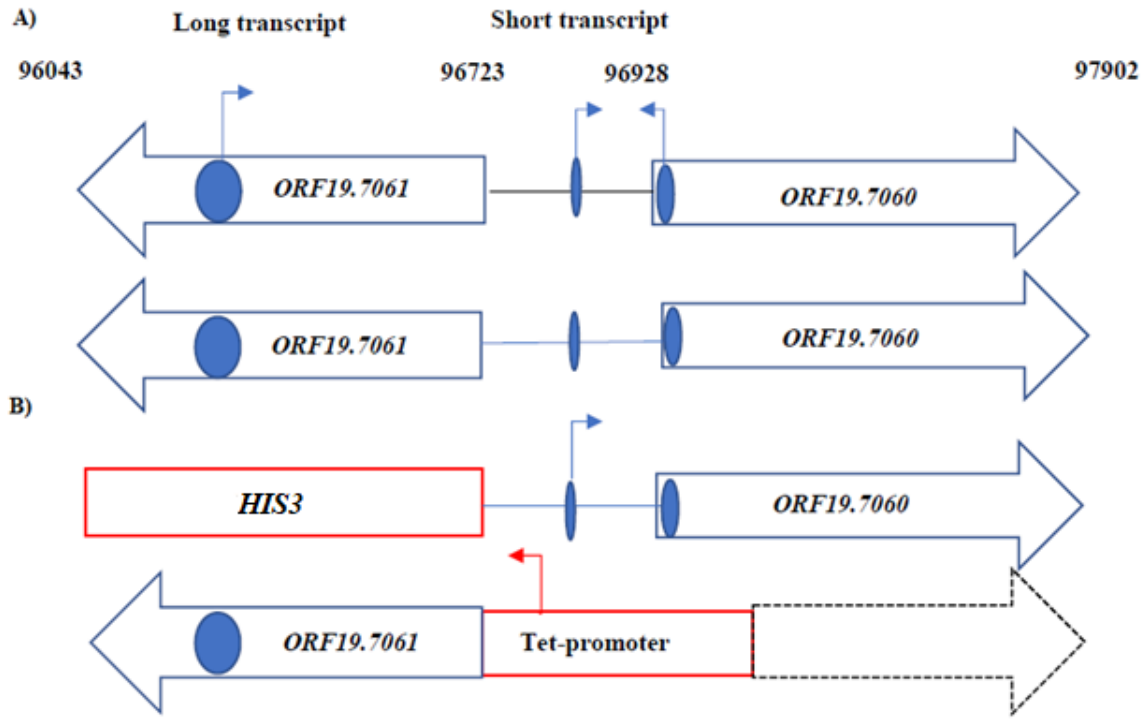

Figure 3.1 A) The architecture of the *ORF19.7061* and *ORF19.7060* genomic region. Transcript start sites are shown as blue ovals; the size of the oval represents the variation in the observed transcript initiations [74]. Numbers represent the genomic positions of the beginning and ends of the two *ORFs.ORF19.7060* has two transcript initiation sites, a long transcript expressed in white cells that starts within *ORF19.7061* around position 96275 and a short transcript expressed in opaque cells that starts between the two genes at genomic position 96790. The transcription starts for *ORF19.7061* was just inside *ORF19.7060* at position 97150. **B)** The structure of the genomic region in the GRACE version 1.0 strain 47H7, where one copy of *ORF19.7061* was replaced with *HIS3* and the endogenous promoter of the other allele was replaced with a *TET*-regulated promoter. The dotted arrow represents the remaining part of *ORF19.7060*.

3.1.1. The architecture of the *ORF19.7060-ORF19.7061* region

The overall structure of the *ORF19.7060-ORF19.7061* region and the original GRACE version 1.0 library deletion shown in Fig.3.1 B establishes the coding region of *ORF19.7061* extends from

position 96723 to position 96043, while the *ORF19.7060* coding region extends from 96928 to 97902. In the white state, the transcript for *ORF19.7060* (termed the long transcript) starts within genomic region 96250-96300; this region is located inside the coding sequence of *ORF19.7061* and so the promoter for the longer, white-specific transcript was removed in the *HIS3* replacement allele of *ORF19.7061*. In the opaque state, the *ORF19.7060* transcript (termed the short transcript) starts at approximately genomic position 96790, which is outside the coding sequence of *ORF19.7061*. However, the promoter replacement of the non-disrupted allele of *ORF19.7061* removes nucleotides 97150 to 96723; this replacement thus removes both the promoter for *ORF19.7061* (after the 97150 genomic region) and the promoter for the short transcript of *ORF19.7060* (96790), as well as part of the start of the coding sequence of *ORF19.7060*. Thus, in white cells, in the absence of the *TET*-regulator, neither *ORF19.7061* nor *ORF19.7060* may be expressed in this strain.

3.1.2. Creation of strain MA10

Initially, to allow a more detailed analysis of the region, I used CRISPR-Cas9 [63, 64] to create a homozygous deletion of both alleles of *ORF19.7061* together with the common 5'-UTR of *ORF19.7060* between the 2 genes, and to replace those sequences with *HIS1*. The replacement started at genomic site 96925, which is 3 nucleotides before the start codon of the *ORF19.7060* and ended at genomic site 95918, which is beyond the stop codon for *ORF19.7061*. (This strategy may disrupt the expression of *ORF19.7060* so the complementation of this strain with both long and short transcripts of *ORF19.7060* was also performed). The structure of the *ORF19.7061/7060* desired replacement construct is shown in Fig.3.2 A. To confirm proper replacement, positive *HIS1* colonies were tested with three different sets of PCR primers. P1 (external region forward primer) and P2 (*HIS1* inside reverse primer) would generate a band of 336 nucleotides in strains where at least one copy of the *ORF19.7061* region was replaced by *HIS1* (Fig.3.2 B). Similarly, PCR using P3 (*HIS1* inside forward primer) and P4 (external region reverse primer) would create a band of 603 nucleotides in strains with a *HIS1* insertion in the *ORF19.7061* region (Fig.3.2 C Due to the very similar sizes, PCR using primers P1and P4 would not generate bands that distinguished between WT and the insertion replacement alleles. Therefore, to distinguish the homozygous replacement allele strains from heterozygotes, I tested P1-P2 and P3-P4 positive colonies with primers P5 (wildtype forward primer) and P6 (wildtype reverse primer) (Fig.3.2 D); these primers

will generate a band of 1100 base pairs in strains that contained a WT allele (Fig.3.2 E). Cells that both lacked the WT band and contained the proper *HIS1* insertion were therefore characterized as containing the homozygous replacement of the *ORF19.7061* region with *HIS1*. This construct was made in strain SN76 [65], and the resulting strain was designated MA10.

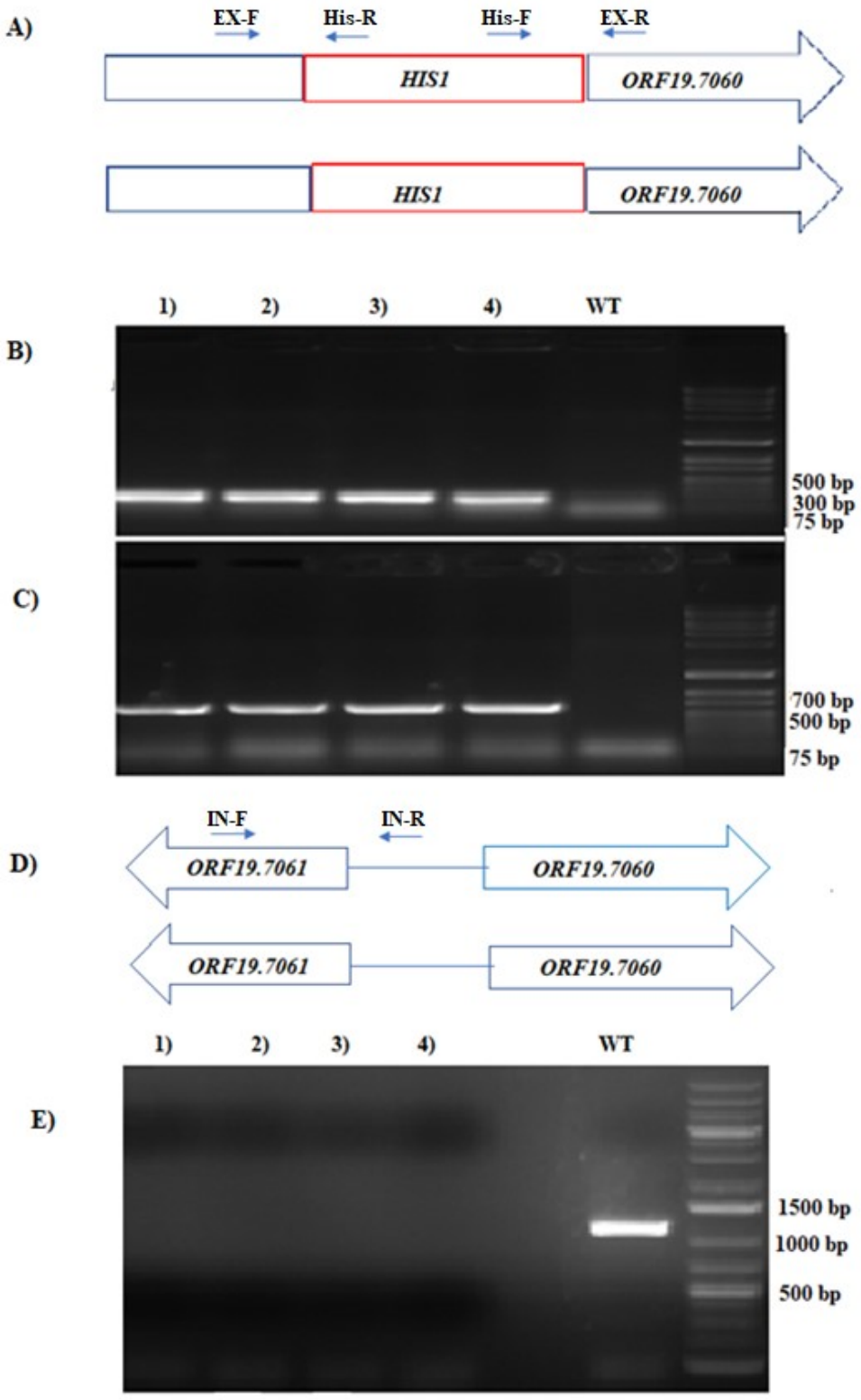

Figure 3.2 A) Structure of the genomic region of *ORF19.7061* and *ORF19.7060* with the *HIS1* gene replacing *ORF19.7061* and the promoter region between the two genes. EX-

F, His-R,His-F and EX-R represent PCR primers for diagnostic amplifications. **B)** Candidate *HIS1+* colonies were tested for insertion of *HIS1* at *ORF19.7061*. Amplification using primers EX-F and His-R will generate a 336 base pair band uniquely in strains with a proper insertion of *HIS1* (Panel B), and amplification using primers His-F and EX-R will generate a PCR product of 603 base pairs uniquely in strains exhibiting the proper insertion of *HIS1* (Panel **C)**. Lanes 1, 2, 3, and 4 show positive colonies, lane 5 shows the wild type control. **D)** The structure of *ORF19.7060* and *ORF19.7061* and the primers IN-F and IN-R defining the wild type locus. The PCR construct expected for strains containing a wild type allele is 1100 bp; this band will be missing in strains that lack a wild type allele. **E)** Colony PCR with primers P5 and P6; WT strain showed the wild type band; strains 1, 2, 3, 4 lacked the wild type allele.

I investigated the phenotypic consequences of the deletion of *ORF19.7061* and its promoter region. Strain MA10 was tested for W/OP switching in the *MTL* **a**/α background by plating on SC-GLcNAc-Phloxin-B plates at 25˚C. As shown in Table 3.1, MA10 generated more than 0.9% opaque colonies, showing that this *MTL* **a**/α strain was de-repressed for white-opaque switching.

Strain	Total Colonies	Opaque Colonies	Ratio%
SN76	3638	0	0%
MA10	1008	10	0.99%
MA110	1218	9.5	0.78%

Table 3.1 The rate of white to opaque switching in the strain MA10 and the strain MA110 compared to the parental strain SN76. MA10 has a deletion in both copies of *ORF19.7061* and both copies of the 5'-UTR of *ORF19.7060*. Strain MA110 is MA10 complemented with an *ORF19.7061* PCR construct driven by the *ACT1* promoter. All the strains are *MTL* ***a****/α.*

I further confirmed that this engineered strain was still heterozygous at the *MTL* locus. PCR reactions using primers P1a and P2a for the *MTL* **a** allele, and P1α and P2α the *MTL*α allele,

established that strain MA10, as well as other strains constructed as part of this study, remained heterozygous at *MTL* (Fig.3.3).

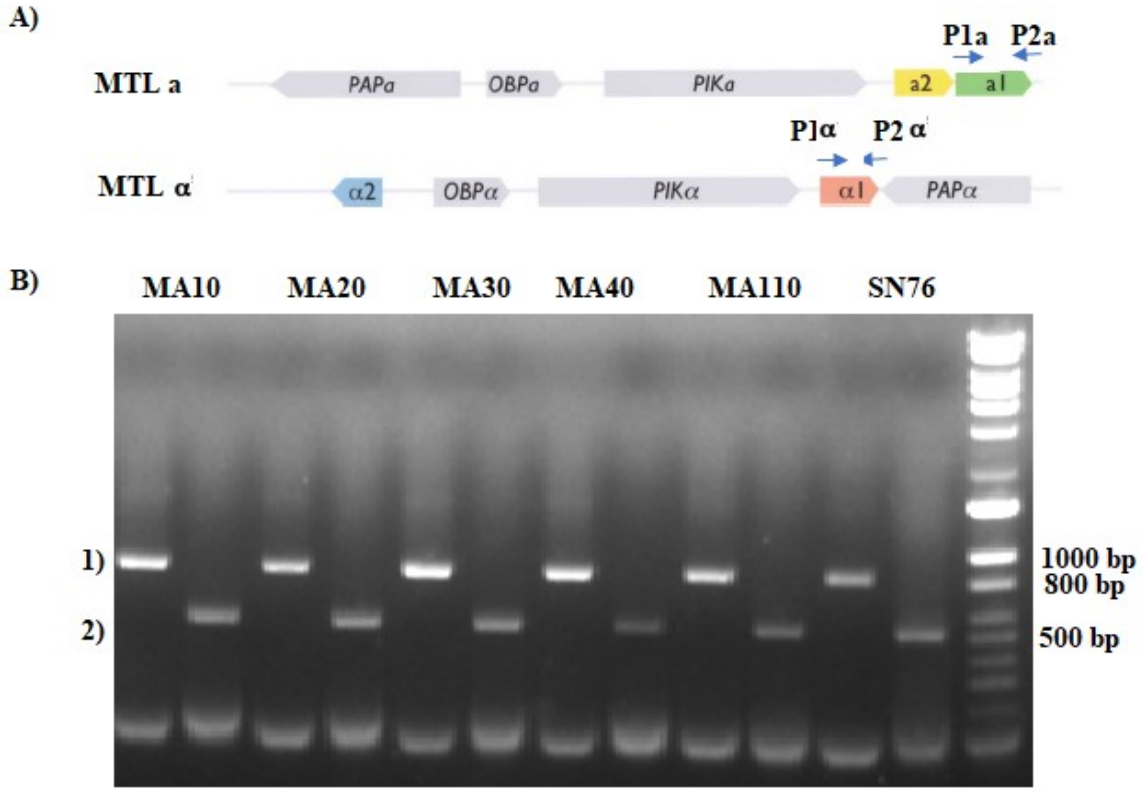

Figure 3.3 **A)** Structure of the *MTL* locus showing *MTL* ***a*** and *MTLα* and the primers designed to detect these two genes [38]. **B)** Colony PCR to detect the *MTL**a**1* and *MTLα1* genes; Band 1) is 828 bp and defines *MTL* **a**, Band 2 is 516 bp and defines *MTLalpha*.

ORF19.7061 showed considerable protein similarity to gene *YFH7* of *S. cerevisiae*, which encodes a putative kinase from the subfamily of P-loop kinases that is annotated as a uridine kinase; in *S. cerevisiae* deletion of *YFH7* modifies sensitivity to wall stress agents [75]. I investigated the response of strain MA10 to the cell wall stressors Calcofluor white (CFW) and Congo red. As shown in Fig.3.4 B and C, strain MA10 showed increased resistance to the effects of both Calcofluor white and Congo red. Thus, MA10 showed two distinct phenotypes when compared to the parental strain SN76; white-opaque switching in a *MTL* **a**/α background, and resistance to agents that cause cell wall stress.

I next investigated whether replacing the wild type copy of *ORF19.7061* could complement these phenotypes by introducing a full-length copy of *ORF19.7061* into the *RP10* locus. Strain MA110 was created by introducing plasmid CIPMA001 (Fig.3.5) into MA10 at the *RP10* locus by targeting it by cleavage with *Stu*I. I compared the behaviour of strain MA10 (Δ/Δ*ORF19.7061*) and strain MA110 (Δ/Δ*ORF19.7061+ORF19.7061*) for both response to cell wall stress and for W/OP switching.

The wall stress resistance of strain MA10 was fully complemented by the insertion of plasmid CIPMA001. Compared to WT, strain MA110 in fact showed increased sensitivity to CFW, and showed similar sensitivity to Congo Red; for both drugs the complemented strain reverted the resistance phenotype caused by the deletion of *ORF19.7061* and the region between *ORF19.7061* and *ORF19.7060* (the 5'-UTR of *ORF19.7060)*. This confirms the functionality of the *ACT1* driven *OFR19.7061.*

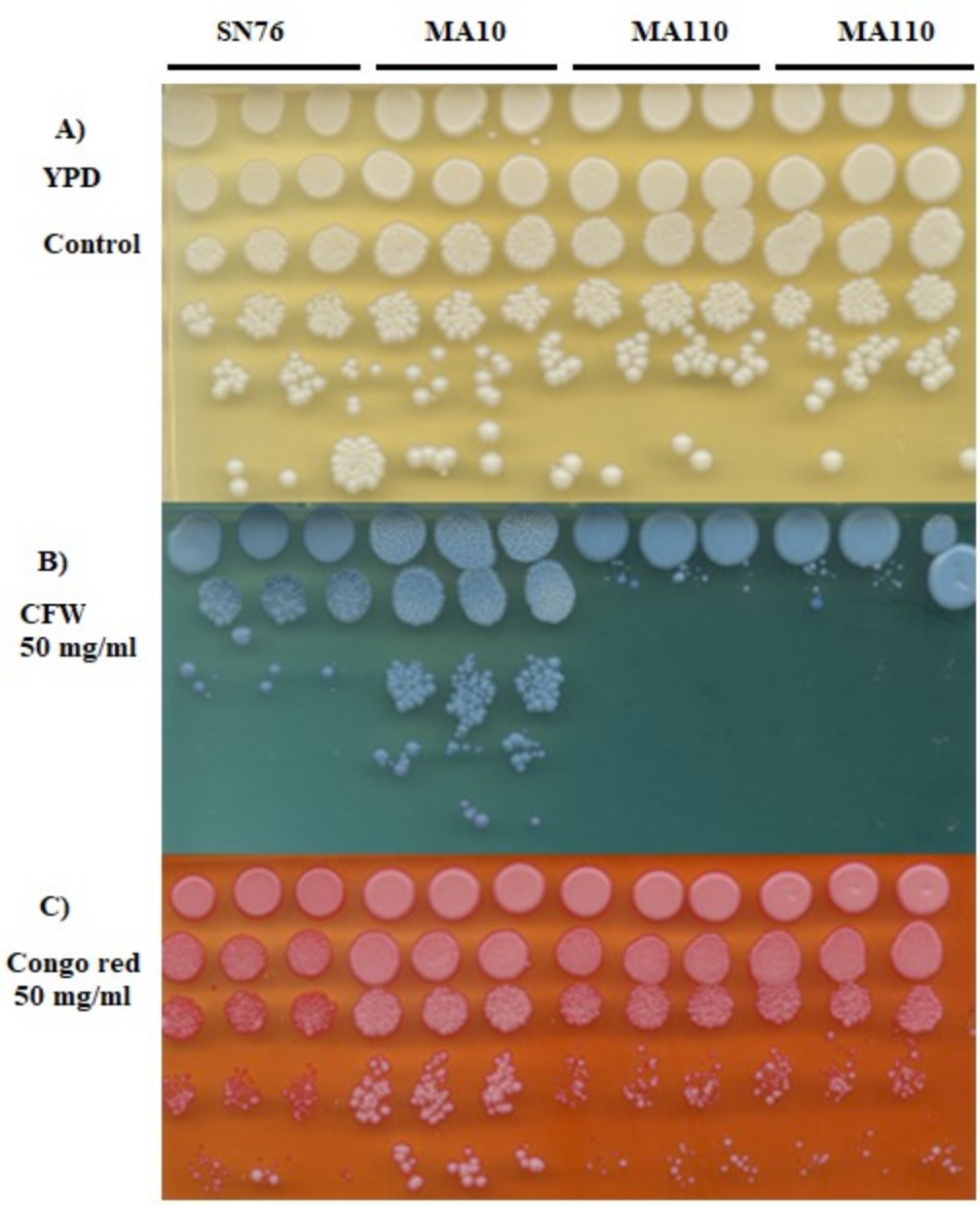

Figure 3.4 Phenotypic assays for response to Calcofluor white and Congo Red **A)** Positive control on YPD agar plate. Triplicates of the strains under investigation were spotted in a series of 10-fold dilutions from top to bottom. **B)** Same samples and dilution protocol grown on plates with 50mg/ml Calcofluor white **C)** Same samples and dilution protocol grown on plates with 50mg/ml Congo Red.

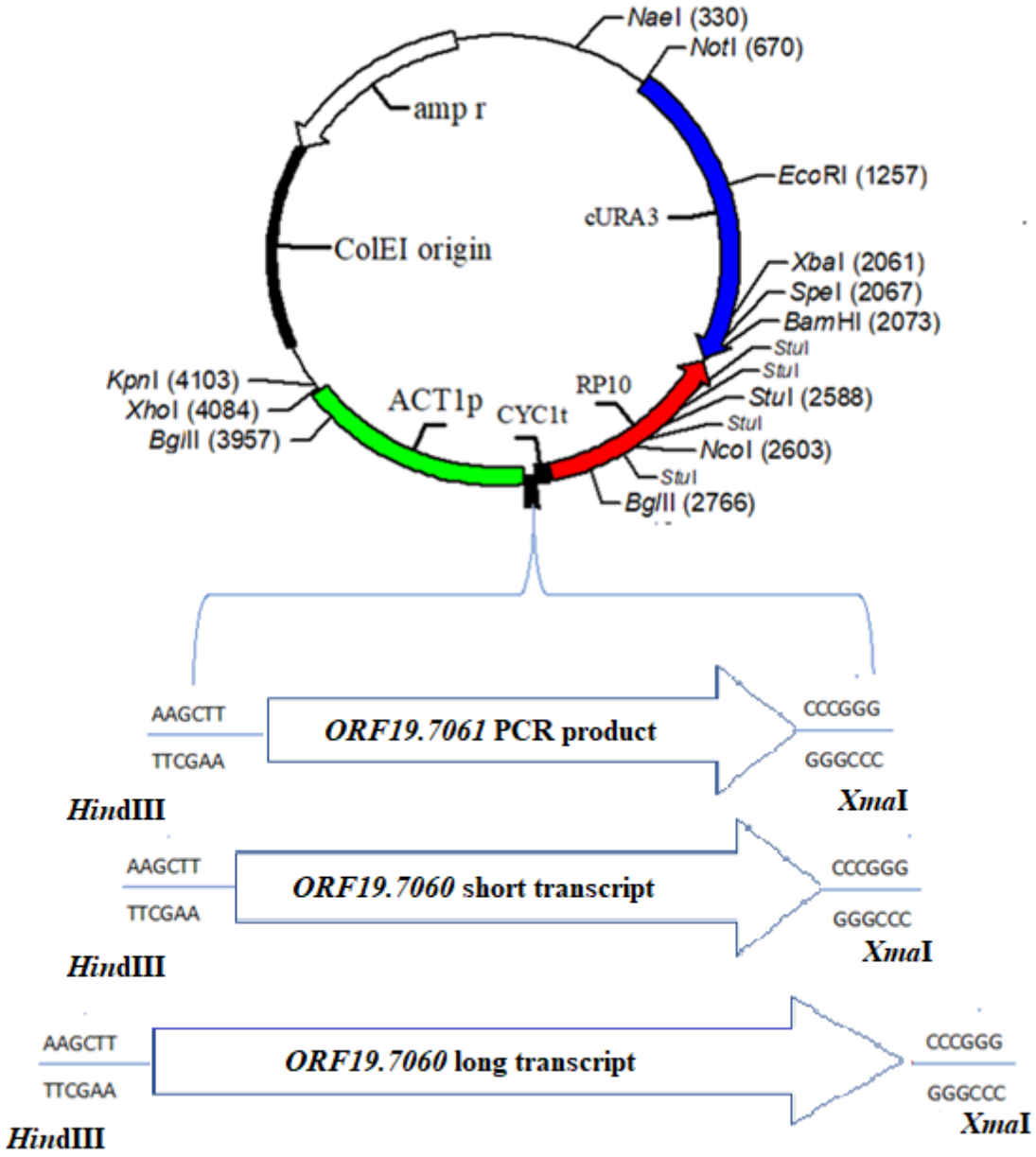

Figure 3.5 The CIP plasmid modified by insertion of either *ORF19.7061* or the white or opaque transcripts of *ORF19.7060* to place the genes under control of the *ACT1* promoter. Restriction enzyme sites (*Hin*dIII and *Xma*I) used to insert the PCR constructs were added to the PCR primers. The plasmids contain the *AMP* gene for *E. coli* selection, c*URA3* for selection in *C. albicans*, and a region of homology to the *RP10* locus of *C. albicans* for directed integrations.

The W/OP switching phenotype was also assessed in strain MA110. Intriguingly, as can be seen in Table 3.1 and Fig.3.6, the introduction of the *ORF19.7061* did not repress the W/OP transition in this strain. The *MTL* **a**/α strains MA10 and the complemented strain MA110 both showed similar frequencies of W/OP switching. This experiment established that although strain MA110 has a functional *ORF19.7061* capable of complementing the wall stress phenotype of the parent MA10, it continues to switch into the opaque phase in the *MTL* **a**/*α* background (Fig.3.6 B). This result is consistent with a previous observation that inactivation of *ORF19.7061* by insertion of a nonsense mutation into the coding sequence of the gene did not de-repress W/OP switching in the *MTL* **a**/*α* background [75]. Therefore, both lines of evidence suggest that the W/OP switching phenotype of either the GRACE version 1.0 mutant or the Δ/Δ*ORF19.7061* strain MA10 was not the result of loss of function of *ORF19.7061*. However, both results are consistent with the adjacent gene *ORF19.7060* and the 5'-UTR of *ORF19.7060* being implicated in the control of W/OP switching, as both mutants that de-repress W/OP switching disrupt the structure of the 5'-UTR of *ORF19.7060* in common between *ORF19.7060-ORF19.7061*. However, independent insertion of the missing region at the RP10 locus did not complement the switching phenotype.

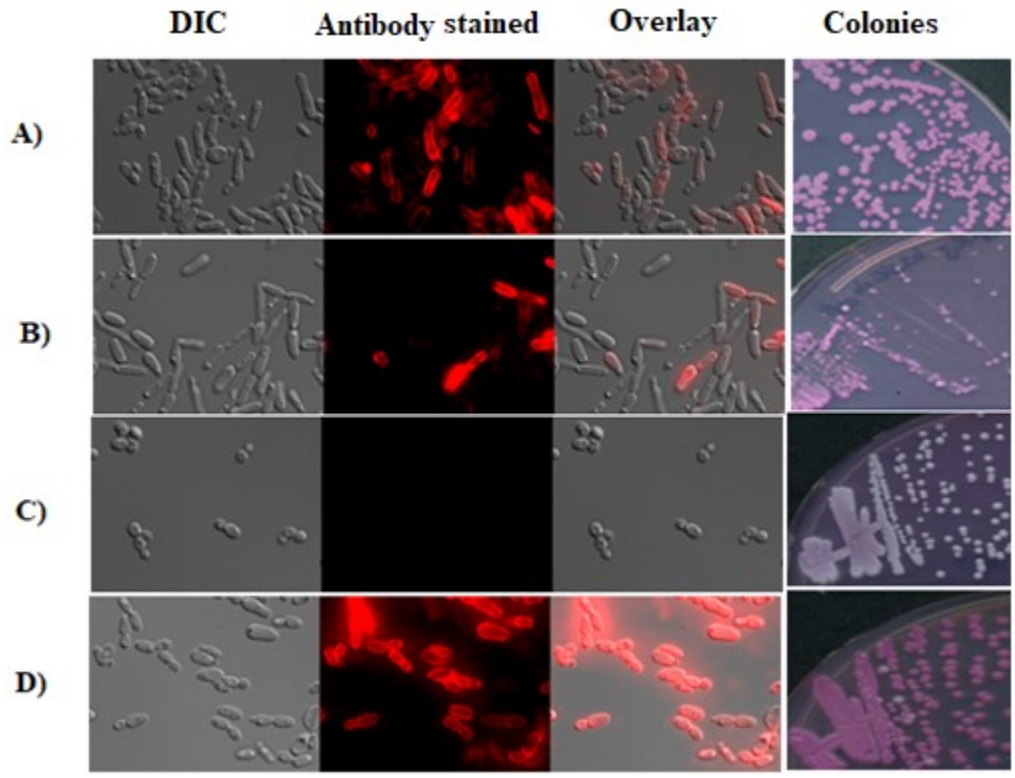

Figure 3.6 Cell and colony characteristics of specified strains. Cells from positive phloxine B staining colonies grown at 25 °C for 4-6 days were assessed microscopically

and photographed with a Leica DM6000 fluorescence microscope at 630X magnification. Cells were analyzed for cell morphology (DIC), for staining with the opaque-specific antibody F223-5E1-1 with Texas red conjugated goat anti-mouse antibody as the secondary antibody (Antibody stained), and by overlay of the images (Overlay) The phloxine B staining colonies were also streaked for single colonies on SC-GlcNAc plus phloxine B agar medium (Colonies).

A) Strain MA10 *MTL* **a***/α*.

B) Strain MA110 *MTL* **a***/α*

C) Strain SN76 *MTL* **a***/α* parental strain as negative control

D) Strain 3745 **a**/**a** as positive control.

3.1.3. Homozygous mutants of *ORF19.7060* undergo the white-opaque transition

I next disrupted both alleles of *ORF19.7060* and analyzed the phenotypic consequences of this mutation. Both copies of the gene in strain SN76 [65] were replaced with *HIS1* using the transient CRISPR protocol [63, 64], to create strain MA20 (*MTL* **a***/α* Δ/Δ*ORF19.7060*). In this strain *HIS1* is inserted from nucleotide 96928 to 97902 to replace the entire coding sequence of *ORF19.7060.* Fig.3.7 displays the colony PCRs that were performed to confirm the transformation. Strain MA20 was analyzed for W/OP switching in the *MTL* **a**/α background by plating on SC-GLcNAc-phloxine-B plates at 25˚C and showed an increase in the rate of W/OP switching from undetectable in SN76 to 0.8% in MA20.

I modified strain MA20 with plasmids containing the long (CIPMA003) and short (CIPMA002) transcripts of the *ORF19.7060* driven by *ACT1* promoter (Fig. 3.4). The plasmids were inserted at *RP10* in strain MA20 to construct strains MA220 and MA230. The successful transformants were still capable of W/OP switching, and thus constructs containing either the long or the short transcripts of *ORF19.7060* did not block the W/OP transition (Fig.3.8 B & C). This result encouraged me to further investigate the 5'-UTR of *ORF19.7060* and specifically the region which causes de-repression of the W/OP transition in *MTL* **a***/α* strain even in a heterozygous state.

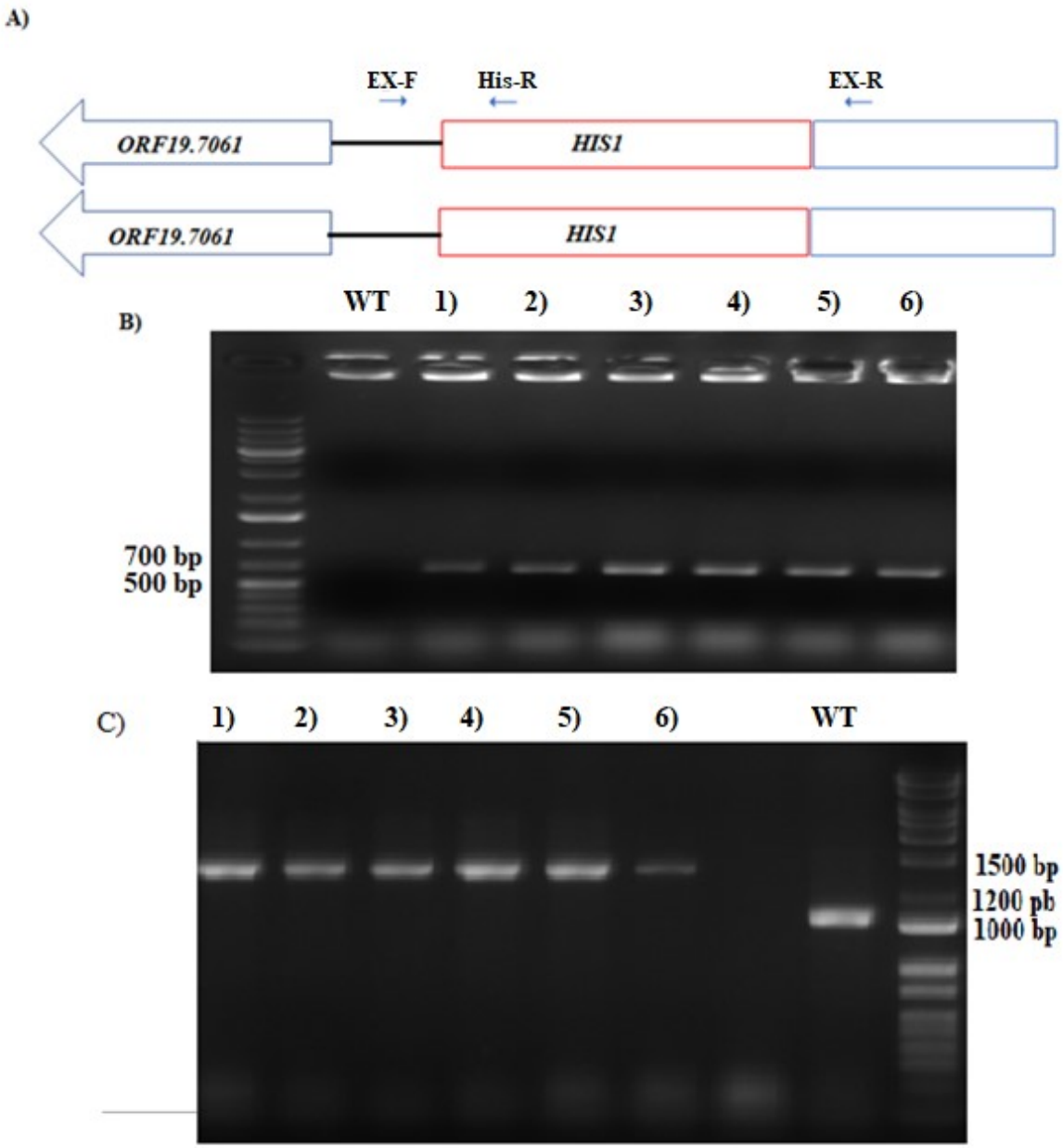

Figure 3.7 Structure of the genomic region of *ORF19.7061* and *ORF19.7060* with the *HIS1* gene replacing *ORF19.7060*. EX-F, His-R and EX-R represent PCR primers for diagnostic amplifications. **B)** Candidate *HIS1*+ colonies were tested for insertion of *HIS1* at *ORF19.7060*. Amplification using primers EX-F and His-R will generate a 617 base pair band uniquely in strains with a proper insertion of *HIS1* (Panel B), C) The structure of *ORF19.7060* and *ORF19.7061* and the primers EX-F and EX-R will generate the band 1137 base pair in wild type and the band 1575 base pair in mutant strain in panel C.

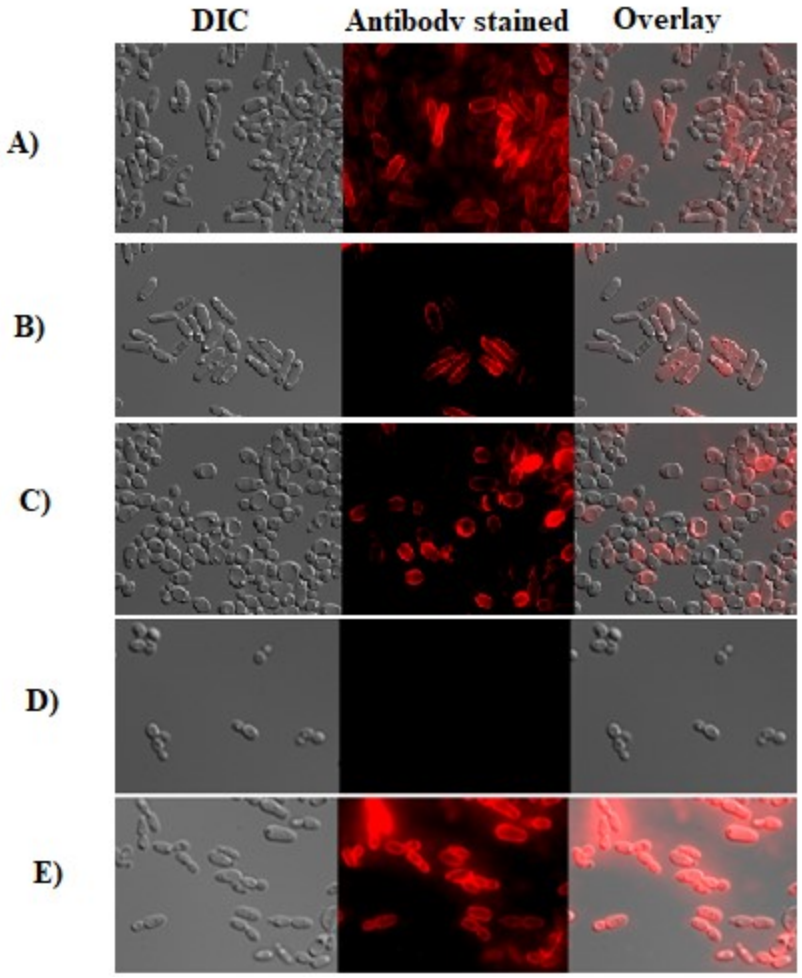

Figure 3.8 Cell characteristics of specified strains. Cells from positive phloxine B staining colonies grown at 25 °C for 4-6 days were assessed microscopically and photographed with a Leica DM6000 fluorescence microscope at 630X magnification. Cells were analyzed for cell morphology (DIC), for staining with the opaque-specific antibody F223-5E1-1 with Texas red conjugated goat anti-mouse antibody as the secondary antibody (Antibody stained), and by overlay of the images (Overlay).

A) Strain MA20 **a**/α.

B) Strain MA220 **a**/α (MA20 complemented with the *ORF19.7060* short transcript)

C) Strain MA230 **a**/α (MA20 is complemented by *ORF19.7060* long transcript

D) SN76 **a**/α negative control.

E) 3745 **a**/**a** positive control.

3.1.4. A heterozygous mutant of *ORF19.7060* undergoes the white-opaque transition.

I next deleted a single copy of *ORF19.7060* and replaced it by *HIS1* to create the heterozygous mutant MA30 Fig.3.9 B shows the colony PCR performed to confirm the transformation. This strain was assessed for W/OP switching in the *MTL* **a**/α background. As shown in Table 3.2, the heterozygous deletion of *ORF19.7060* increased the rate of W/OP switching from undetectable in SN76, to 0.87% in MA30. This result established that the loss of a single copy of *ORF19.7060* allows W/OP switching in the *MTL* **a**/α background that normally restricts this transition.

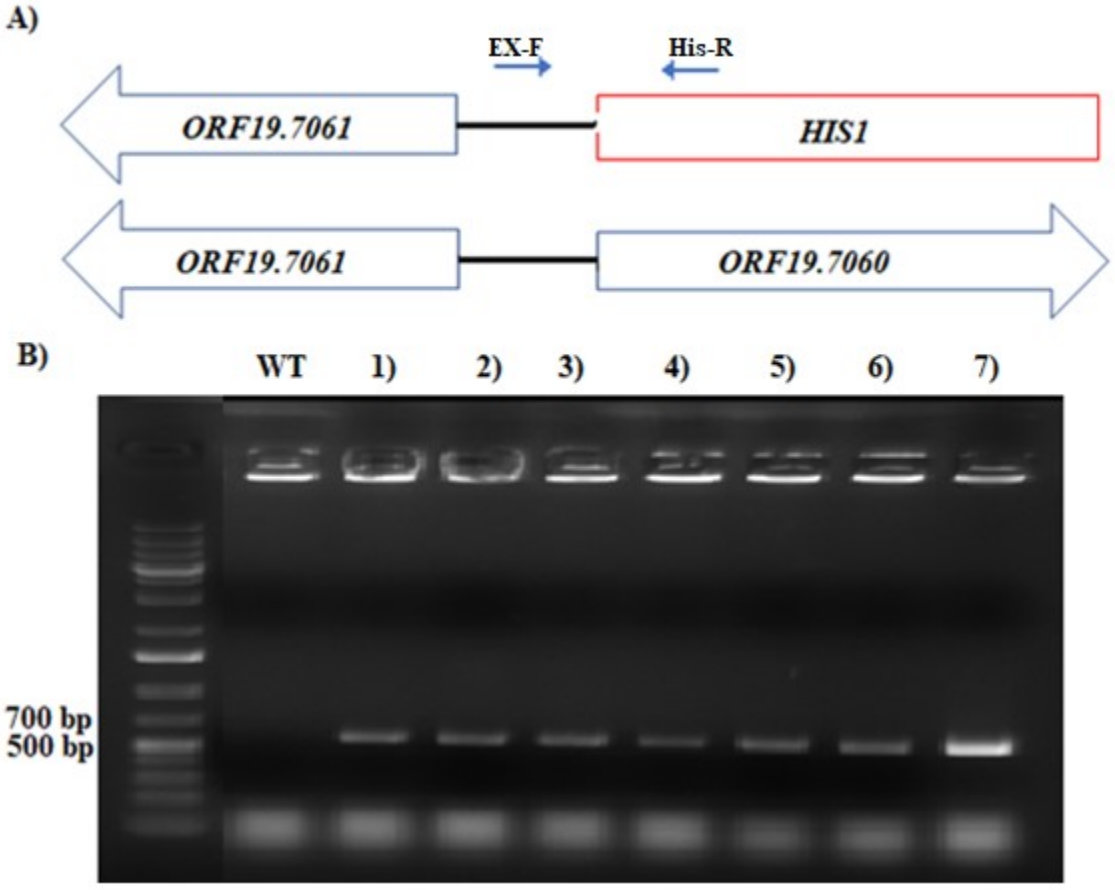

Figure 3.9 A) Structure of the genomic region of *ORF19.7061* and *ORF19.7060* with the *HIS1* gene replacing *ORF19.7060* and 5'-UTR of *ORF19.7060* which contains *ORF19.7061* and the region between the two genes. EX-F and His-R represent PCR primers for diagnostic amplifications. **B)** Candidate *HIS1+* colonies were tested for insertion of *HIS1* at *ORF19.7060*. Amplification using primers EX-F and His-R will

generate a 617 base pair band uniquely in strains with a proper insertion of *HIS1* (Panel B). This band will not be formed in a wild type strain.

3.1.5. Heterozygous mutants of the 5'-UTR of *ORF19.7060* also can undergo the white-opaque transition

Since the deletion constructs in strains MA10, MA20 and MA30 allowed de-repression of the W/OP transition, it was possible that it was not the coding sequences per se within the *ORF19.7060/ORF19.7061* region that were critical for creating the opaque phenotype, rather, it was the change in the genomic context that allowed de-repression of W/OP switching. Therefore, I further investigated the structure of the region by creating a heterozygous mutant of the 5'-UTR of *ORF19.7060* (contains *ORF19.7061* and the common region between these two genes). I deleted the entire 5'-UTR of *ORF19.7060* in one allele in SN76 *MTL* **a**/α that extended from genomic region 96928 to 95918 and replaced it by *HIS1* in a one-step mutagenesis [66], to create strain MA40. I tested MA40 for W/OP switching, which went from undetectable in the parent SN76, to 0.95% in MA40 (Table 3.2 and Fig.3.8 A & B). Thus, removal of only one copy of *ORF19.7061* and 5'-UTR of *ORF19.7060* gene was sufficient to de-repress white-opaque switching.

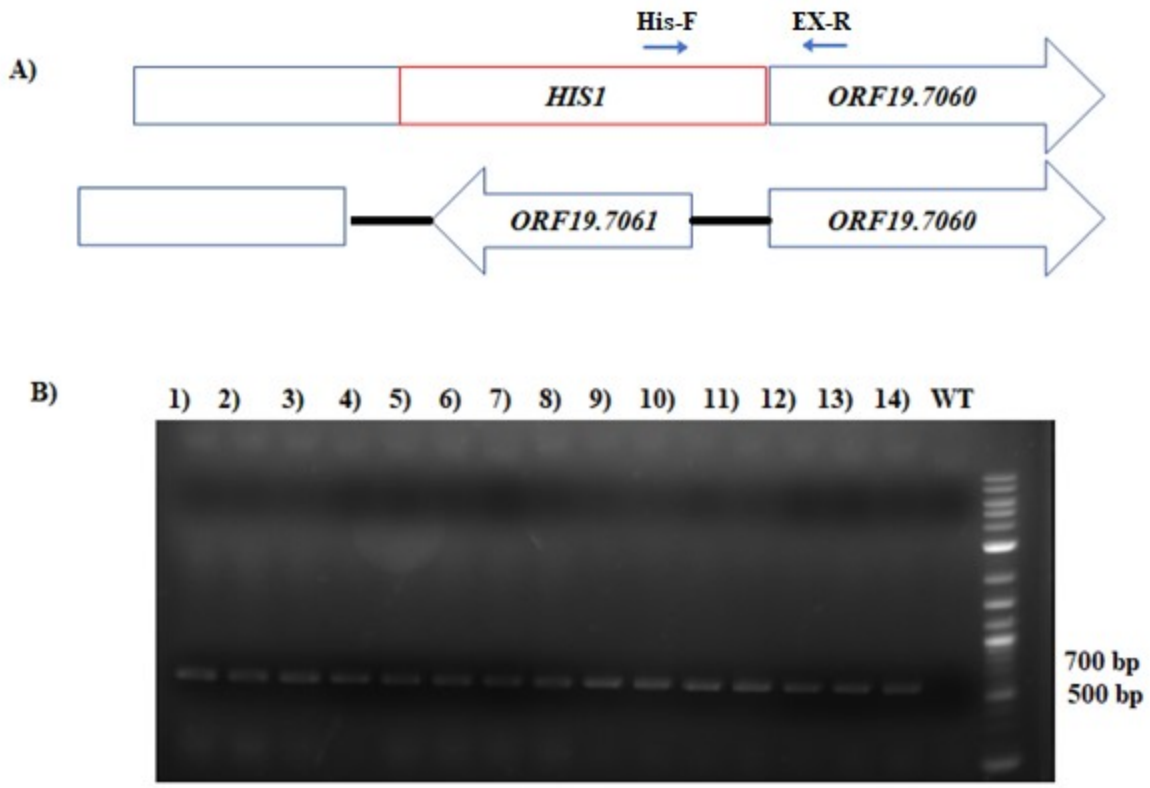

Figure 3.10 A) Structure of the genomic region of *ORF19.7061* and *ORF19.7060* with the *HIS1* gene replacing *ORF19.7061* and the 5'-UTR region between the two genes. His-F and EX-R represent PCR primers for diagnostic amplifications. **B)** Candidate *HIS1*+ colonies were tested for insertion of *HIS1* at *ORF19.7061*. Amplification using primers His-F and EX-R will generate a PCR product of 603 base pairs uniquely in strains exhibiting the proper insertion of *HIS1* (Panel **B)**. This band will not be formed in the wild type strain.

Strain	Total colonies	Opaque colonies	Ratio%
SN76 **a**/α	3638	0	0%
CAI4 **a/a**	2010	70	3.48%
MA20 **a**/α	2060	17	0.8%
MA30 **a**/α	2600	23	0.87%
MA10 **a**/α	2008	19	0.94%
MA40 **a**/α	4424	43	0.97%

Table 3.2 The rate of W/OP switching. Strains MA10, 20, 30 and 40 *MTL* **a**/α were assessed, along with strain SN76 *MTL* **a**/α as the negative control, and strain CAI4 *MTL* **a/a** as the positive control. The ratio of white to opaque switching was calculated from among 500 to 1000 colonies per experiment after 4-7 days incubation at room temperature. The carbon source used was GlcNAc (GLC). Strains were all initiated from white (WH) cells. The ratios are based on at least 3 independent experiments;

3.2 RNA sequencing results revealed differences between strains with homozygous and heterozygous deletion of the entire the 5'-UTR of the *ORF19.7060* region compared with the normal opaque transcriptome.

In wild type cells, the W/OP transition is under control of the master transcriptional regulator *WOR1*; high levels of *WOR1* activate the opaque state while low levels maintain the white state. An approximately 40-fold increase is observed in the *WOR1* transcript levels in the opaque cells relative to white cells [14], and this *WOR1* overexpression regulates the downstream genes of the opaque circuitry. A comparison of white and opaque state cells demonstrated that more than 400 genes were differentially regulated in their expression profiles; 237 genes were up-regulated specifically in the opaque state, while 179 genes were highly expressed in white cells [14].

This white-opaque switching is inactivated in normal *MTL* **a**/α cells because the a1-α2 repressor encoded at the *MTL* locus blocks *WOR1* expression[52]. The white-specific genes that are differentially regulated between these two cell states may play a role in maintaining the cells in the white state. *EFG1* encodes a white-specific transcription factor that plays a critical role in repressing the opaque transition in the *MTL* **a**/α genotype in clinically isolated samples [61], while deletion in other transcription factors (TFs) such as *RFG1* and *BRG1* can de-repress the opaque transition in an *MTL* **a**/α strain [76]. Another study demonstrated that deletion in *SLF2* (a transcription factor) can create the opaque phenotype in *MTL* **a**/α cells in a carbon source dependent manner (GLcNAc as inducer and Glucose as suppressor) in 37˚C and high CO_2 (5%) [62].

I used RNAseq analysis to establish the expression of genes involved in W/OP switching and mating type control in the homozygous and heterozygous deletion of 5'-UTR of *ORF19.7060*, in

strains MA10 and MA40, both of which created a state permissive for W/OP switching in cells that were *MTL* **a**/α. I also analyzed the expression of the transcription factors where deletion created W/OP transitions in *MTL* **a**/α cells [62, 63, 78]. When compared to the control SN76 **a**/α, the opaque cells of strains MA10 and MA40 displayed about 125 genes up-regulated more than 1.5-fold, and the changes were generally consistent with classical opaque transcription expression. In particular, genes such as *WOR1, WOR3, SOD3, OP4, PGA28,* and *PHO89* which are up-regulated in classic opaque-state cells [77], were up-regulated in both MA10 and MA40 cells exhibiting opaque phase characteristics. There are also 86 genes in both data sets that were down-regulated more than 1.5-fold that are also down-regulated in classic opaque cells, such as *ATO6, MNN22, XUT1, WH11,* and *MET3* [77]. However, some interesting variations in gene expression were observed. For instance, there are 49 genes in the MA10 and MA40 data sets that were highly up-regulated but were down-regulated in classic opaque RNA-seq data, including *FMA1, PMS1, CTF5, GCA1,* and *PGA26*. As well, 35 genes were down-regulated in our data that were highly expressed in the standard opaque data set, including *KAR4, SAP4,* and *HWP1* [77].

W/OP switching is normally suppressed by the **a**1-α2 heteromeric repressor in *MTL* **a**/α cells due to the direct repression of *WOR1* expression. In the MA10 and MA40 opaque cell transcriptomes, the expression of *WOR1* is as high as in the control opaque data set. Sequencing of the *MTL* locus of these strains showed the *MTL***a**2 and α1 genes are intact, which suggested that deletion of 5'-UTR of *ORF19.7060* in both MA10 and MA40 may have caused disruption of normal *MTL* regulation of the opaque state.

I therefore investigated *MTL* gene expression in the opaque-state MA40 and MA10 cells. In both MA40 and MA10 *MTL***a***1* was expressed, but the expression of *MTL***a***1* was drastically higher in MA10 which accompanied in this strain with the expression of non-sex genes (*PIKa, OBPa* and *PAPa)* at the *MTL**a*** locus. By contrast, no expression of *MTL***a***2* was detected in either strain MA10 or MA40. Analyzing the *MTLalpha* genes showed that all the non-sex genes at the *MTLalpha* locus (*PIKα, OBPα* and *PAPα*) and *MTLalpha2* were expressed in both MA10 and MA40 data sets and this expression was noticeably higher in strain MA40. Although no expression of *MTLalpha1* was found in strain MA10, this gene had quite a high expression in the strain MA40. This imbalance of the expression at the *MTLalpha* genes and specifically expression of *MTLalpha1* can explain the consequent high expression of some α-specific genes such as *MFα1* and *STE3* which were highly expressed in the strain MA40 due to the expression of *MTLalpha1* as a positive

regulator of the α-specific genes. These expression data for genes at the *MTL* locus are displayed in Fig.3.11. [78].

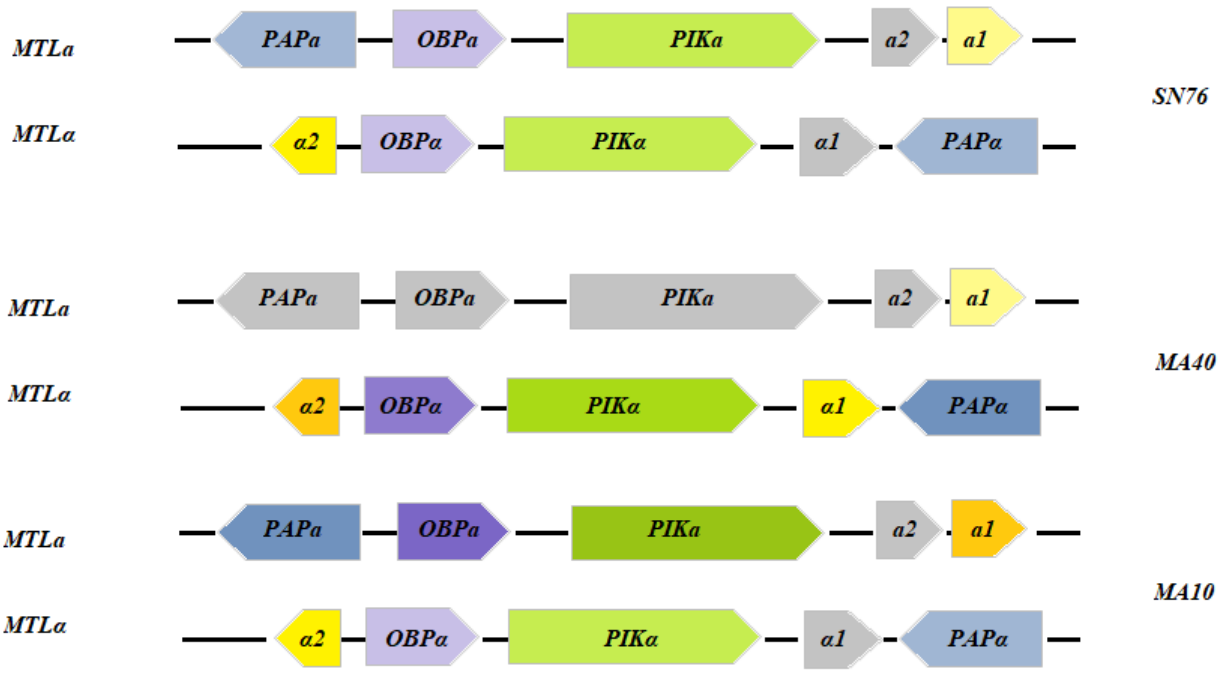

Figure 3.11 Structure of the *MTL* locus showing *MTL***a** and *MTLalpha* in SN76 as a control, strain MA40 and strain MA10. Gray coloring represented the undetectable expression or highly down regulation, green represents the *PIK* gene, violet represents *OBP* gene expression and blue represents the expression of *PAP* genes. Yellow represents the mating genes. The higher expression of the genes is displayed by a darker color and lower expression of the genes is displayed by a lighter color.

Feature	Name	OP/fold change	MA10/fold change	Ma40/fold chang	Feature	Name	OP/fold chang	MA10/fold change	Ma40/fold chang
C1_04050C_A	*MFALPHA*	12.8	0.0	9.2	CR_03890W_A	*WOR3*	6.6	9.4	9.1
C4_03570W_A	*HWP1*	11.9	-3.8	-2.4	C2_06930C_A	*orf19.2247*	6.5	0.5	0.8
C6_01310W_A	*FIG1*	11.3	0.0	0.0	CR_06610W_A	*STE2*	5.7	0.0	0.0
C4_04070C_A	*PGA30*	11.3	5.4	6.3	C4_06480C_A	*CEK1*	5.2	0.7	1.2
C1_06160W_A	*orf19.2429*	11.0	0.0	0.0	C4_04080C_A	*PGA31*	5.0	9.8	4.8
C1_05620C_A	*STE3*	10.9	0.0	8.3	C5_04140W_A	*orf19.3897*	4.5	5.5	5.5
C4_03470C_A	*ECE1*	10.9	-1.9	1.2	C3_05170W_A	*WOR2*	4.1	-0.6	-0.9
CR_04900C_A	*PGA39*	10.5	0.0	3.4	C5_00540C_A	*AGA1*	4.1	2.8	3.4
C2_08210C_A	*MFA1*	9.9	0.0	0.0	C5_03430W_A	*orf19.2638*	4.1	-2.0	1.3
C2_00460W_A	*SAP30*	9.7	0.0	0.0	C2_09130C_A	*IFF6*	3.9	8.9	8.9
C1_10150W_A	*WOR1*	9.7	10.9	10.0	C1_02990C_A	*XOG1*	3.6	-1.5	1.0
C2_09800C_A	*orf19.1370*	9.6	4.1	4.9	C7_00770W_A	*orf19.7042*	3.6	2.3	-0.5
C6_02510C_A	*ASG7*	9.4	0.0	0.0	C1_07980C_A	*orf19.5069*	3.4	6.7	4.1
C1_11630C_A	*FUS1*	9.3	-1.9	-0.7	C4_02740W_A	*orf19.2724*	3.3	2.4	0.8
C6_03500C_A	*SAP4*	9.0	-5.4	-4.1	C4_06890W_A	*ARR3*	3.1	2.9	2.7
C1_06220C_A	*orf19.1827*	8.9	0.0	0.0	C5_02630C_A	*MNN1*	3.0	8.9	8.3
C1_13440C_A	*orf19.4972*	8.7	10.2	9.4	C2_02610C_A	*HGT20*	2.8	4.8	5.1
C3_06510C_A	*HST6*	8.7	1.2	0.0	CR_00210W_A	*ALK2*	2.7	1.1	1.7
C4_04790W_A	*FAV1*	8.7	3.9	0.0	C7_00110W_A	*SOD3*	2.7	10.2	9.7
C5_04380C_A	*orf19.3924*	8.7	4.0	3.5	C5_01360W_A	*CFL4*	2.7	-3.8	2.9
C1_11340W_A	*PRM1*	8.6	2.8	2.1	C1_11480W_A	*PHO84*	2.5	-2.9	-0.9
C1_06370C_A	*PBR1*	8.5	2.5	1.4	C5_05220W_A	*CAG1*	2.5	-0.4	4.4
C7_00480W_A	*FGR2*	8.4	5.3	7.3	C4_01360W_A	*PGA53*	2.3	3.0	2.6
C4_01940W_A	*PHO89*	8.4	6.8	7.1	C4_06820C_A	*CZF1*	2.1	1.8	1.7
C2_02220C_A	*orf19.1539*	8.2	3.9	2.9	C5_04130C_A	*CHT2*	2.0	1.3	2.0
C2_04470W_A	*ADH3*	7.8	9.0	7.6	C6_03790C_A	*HGT10*	1.9	-5.9	-4.8
C1_13080W_A	*OP4*	7.6	5.5	5.4	C7_01730C_A	*STE18*	1.7	-0.9	2.2
C1_10430W_A	*PHO8*	7.4	6.4	6.6	C2_04210W_A	*STE4*	1.5	1.2	8.2
C6_03600C_A	*orf19.5728*	7.0	7.9	9.0	C3_06000W_A	*AHR1*	1.3	-0.9	-2.8
CR_05940W_A	*CEK2*	7.0	4.5	6.1	C5_05430W_A	*PEX4*	0.9	2.2	-0.7
C7_03110W_A	*PGA28*	6.9	10.7	9.2	C3_07020W_A	*SSN6*	-0.9	0.4	0.0
					C3_07730W_A	*wor4*	-1.9	1.1	0.7

Table 3.3 60 genes involved in the W/OP transition that were up-regulated in the true opaque data set were compared to the MA10 and MA40 RNA seq results. RNA-Seq results for the strains MA10 and MA40 *MTL* **a**/*α.* Opaque colonies were purified by streaking a single colony over the GLcNAc plate and the stable opaque colonies were selected for RNA extraction. The samples MA10 and MA40 *MTL* **a**/*α* were normalized against the WT SN76 **a**/α strain. The true opaque RNA expression results were normalized against white locked cells containing a *Wor1* deletion. This table also displays the heat map for the gene expression in classic opaque and both strains MA10 and MA40.

Feature	Name	Op/fold change	MA40/fold change	MA10/fold change
C4_03570W_A	*HWP1*	11.9	-2.4	-3.8
C6_03500C_A	*SAP4*	9.0	-4.1	-5.4
C4_03520C_A	*RBT1*	8.6	-3.2	-3.9
C4_01800W_A	*N/A*	6.0	-1.9	-2.1
CR_02330C_A	*KAR4*	5.4	-3.4	-1.9
C2_03720W_A	*PGA16*	4.2	-2.4	-3.8
C7_00430W_A	*FRE7*	4.0	-2.2	-3.5
C1_06870C_A	*N/A*	3.8	-3.0	-3.9
CR_03840C_A	*N/A*	3.4	-1.9	-2.0
C1_04470C_A	*N/A*	3.3	-5.7	-3.0
C6_01400W_A	*SGE13*	3.2	-2.1	-4.7
C1_08170C_A	*BUL1*	3.1	-3.7	-3.5
C4_02230C_A	*HQD2*	3.1	-4.2	-1.7
C3_00320W_A	*RHR2*	3.0	-3.1	-1.9
C3_03800W_A	*PTR22*	2.8	-3.0	-3.0
C4_03820C_A	*HRQ2*	2.6	-2.9	-1.6
C2_06970W_A	*AAH1*	2.4	-4.4	-2.9
C3_02060W_A	*N/A*	2.4	-3.4	-4.7
C1_04500W_A	*ICL1*	2.3	-1.7	-3.4
C1_05830W_A	*N/A*	2.2	-3.6	-5.0
CR_10460W_A	*N/A*	2.2	-3.1	-2.4
C4_04030W_A	*JEN2*	2.2	-3.2	-4.1
C2_08055W_A	*RPR1*	2.2	-1.9	-1.9
C5_00450C_A	*IFG3*	2.1	-3.2	-2.7
C4_06120W_A	*GDH3*	2.0	-2.0	-3.0
C6_03790C_A	*HGT10*	1.9	-4.8	-5.9
C6_03230W_A	*ARG3*	1.8	-5.6	-5.7
C1_00050C_A	*N/A*	1.8	-2.1	-5.3
C3_04340W_A	*ATF1*	1.8	-4.5	-3.3
C6_00790C_A	*CTR1*	1.8	-3.3	-4.3
C3_06220C_A	*OAC1*	1.6	-2.3	-4.0
C5_03530C_A	*N/A*	1.6	-2.1	-2.4
C6_02400W_A	*N/A*	1.5	-2.7	-5.4
C2_04810W_A	*HIS3*	1.5	-2.1	-2.4
C3_05590C_A	*BAT22*	1.5	-3.6	-3.4

Table 3.4 35 genes were up-regulated in the true opaque data set and down regulated in both MA10 and MA40. RNA-Seq results for the strains MA10 and MA40 *MTL* **a**/*α* the opaque colonies were purified by streaking a single colony over the GLcNAc plate and

the stable opaque colonies were selected for the RNA extraction. The samples MA10 and MA40 *MTL* **a**/*α* were normalized against the WT SN76 **a**/α strain. The true opaque RNA expression results were normalized against a white locked cell containing a *Wor1* deletion. Genes that were down regulated in both strains compared to the true opaque data set are shown. RNA-Seq for MA10 and MA40 were compared to the classic opaque data expression.This table also displays the heat map for the gene expression in classic opaque and both strains MA10 and MA40.

Feature	Name	OP/fold change	MA40/fold change	MA10/fold change
C2_08300C_A	*N/A*	-6.7	2.9	8.4
C3_06940W_A	*N/A*	-6.1	1.6	3.0
CR_09060W_A	*N/A*	-5.7	2.4	3.8
C7_02880C_A	*LIP9*	-4.3	2.2	2.1
C1_08790W_A	*TPO3*	-4.3	2.5	2.2
C1_12470W_A	*N/A*	-3.6	2.2	2.9
C1_06830W_A	*N/A*	-3.6	2.1	2.7
C1_09060C_A	*N/A*	-3.3	2.5	2.0
C1_07770W_A	*FGR6-3*	-3.1	3.8	3.4
CR_08250C_A	*HSP104*	-3.0	1.5	3.5
C2_06620W_A	*N/A*	-2.7	4.2	2.8
C1_10290W_A	*GCA1*	-2.7	4.5	4.9
CR_00010C_A	*N/A*	-2.6	2.0	4.0
C1_02210W_A	*N/A*	-2.6	1.5	2.1
C1_10400C_A	*FGR41*	-2.6	2.6	2.6
C7_00760C_A	*N/A*	-2.5	5.1	5.3
C1_05760C_A	*PGA26*	-2.5	4.4	3.9
C1_05220C_A	*N/A*	-2.3	2.9	2.0
C4_00370W_A	*HOF1*	-2.3	2.2	2.0
C2_08490W_A	*DSE1*	-2.2	1.6	2.0
C2_01380W_A	*PLB4.5*	-2.2	2.2	2.6
CR_08270W_A	*N/A*	-2.1	1.6	4.4
C2_08820C_A	*SPO11*	-2.1	1.8	5.3
C6_00750C_A	*PGK1*	-2.1	1.7	2.1
C2_06760C_A	*N/A*	-2.0	5.3	3.0
CR_06920W_A	*N/A*	-2.0	3.9	3.7
C6_02130C_A	*CTF5*	-2.0	6.0	4.1
C2_10310C_A	*KIP2*	-2.0	3.1	3.1
C2_09470C_A	*PMS1*	-1.9	6.4	4.4
C1_13160W_A	*PSA2*	-1.9	4.2	5.3
C4_02440C_A	*PGA38*	-1.9	1.8	1.7
C1_02580W_A	*HNM4*	-1.8	2.1	2.6
C1_11990W_A	*N/A*	-1.8	4.5	3.4
C1_08150C_A	*N/A*	-1.8	3.0	3.9
C3_05390C_A	*GPI1*	-1.8	3.7	3.9
C2_00860C_A	*N/A*	-1.8	5.5	4.5
CR_07460C_A	*N/A*	-1.8	2.4	2.2
C4_03990C_A	*N/A*	-1.7	1.8	2.8
CR_08310C_A	*N/A*	-1.7	4.3	2.1
CR_06740W_A	*N/A*	-1.7	2.7	1.7
C7_01690W_A	*N/A*	-1.7	2.4	4.1
C1_04940C_A	*N/A*	-1.7	1.6	3.2
C1_11270W_A	*N/A*	-1.6	2.3	4.6
C3_01070C_A	*N/A*	-1.6	2.6	1.6
C1_08500C_A	*ENO1*	-1.6	2.1	2.7
CR_05840W_A	*N/A*	-1.6	3.0	1.6
C1_04450C_A	*FMA1*	-1.5	7.0	6.4
C3_06810W_A	*N/A*	-1.5	2.0	2.5
C4_04910C_A	*SPC34*	-1.5	3.4	2.4

Table 3.5 49 genes were up-regulated in both MA10 and MA40 strain that were down regulated in the true opaque data set. RNA-Seq results for the strains MA10 and MA40 *MTL* **a**/*α.* The opaque colonies were purified by streaking a single colony on a GLcNAc plate and stable opaque colonies were selected for the RNA extraction. The samples MA10 and MA40 *MTL* **a**/*α* were normalized against the WT SN76 **a**/α strain. The true opaque RNA expression results were normalized against a white locked cell containing a *Wor1* deletion. Genes that were up-regulated in both strains compared to the true opaque

data set are presented. RNA-Seq for both MA10 and MA40 were compared to the classic opaque data expression. This table also displays the heat map for the gene expression in classic opaque and both strains MA10 and MA40.

The expression of the specific transcription factors which their deletion can create the opaque phenotype in the *MTL* **a**/α genotype were also investigated. *EFG1,* the white state regulator, was down regulated in both MA10 and MA40. Both data sets also displayed the downregulation of *RFG1*. The expression data also showed that both strains MA10 and MA40 had a drastic low expression of *SFL2* even compared to the classic opaque data expression. However, *BRG1* had noticeable expression in MA40 and high expression in MA10, although the 2-fold change in expression of *BRG1* was consistent with the expression of this gene in a classic opaque data set. All the expression data connected to these genes are displayed in Table 3.6.

Gene Name	OP/fold change	MA10/fold change	MA40/fold change
EFG1	-2.0	-0.28	-2.0
RFG1	0.7	-0.9	-0.8
BRG1	2.7	2.4	0.12
SFL2	-1.9	-9.4	-6.1

Table 3.6 The expression of specific transcription factors in MA10 and MA40 compared to classic opaque expression.

3.3 Creating sequential deletions in the 5'-UTR of *ORF19.7060*

To determine which region of the 5'-UTR of *ORF19.7060* was responsible for the opaque switching phenotype and to understand how critical this region was, serial deletion sets within the 5'-UTR of *ORF19.7060* were constructed (Fig.3.12). Since the heterozygous mutant in the 5'-UTR of *ORF19.7060* underwent W/OP transition in the strain MA40, a series of heterozygous deletions were made in strain SN76 **a**/α. Both copies of the *ORF19.7060* gene and one copy of the *ORF19.7061* were intact and only one copy of the 5'-UTR of *ORF19.7060* was disrupted. The first

deletion removed the genomic region from 96778 to 95918 and replaced it with *HIS1*. Each successive deletion was about 80-150 nucleotides smaller than the previous one, and all regions were replaced by *HIS1*. These mutant strains were designated MA201 to MA208 5'-UTR of *ORF19.7060-No1-8+/Δ* (Fig.3.12). After mutation confirmation, all deletion mutants were streaked on SC-GLcNAc plates and monitored at room temperature for 7 days to assess their ability to undergo the W/OP transition. All the heterozygous deletions showed the formation of pink colonies typical of opaque cells (Fig.3.13 A, B&C, 3.14 A, B, C&D and 3.15 A&B all colonies). Confirmation of the true opaque phenotype was assessed by immunofluorescence microscopy which allowed us to analyze the mutant strains accurately at the cellular level (Fig.3.13 A, B&C, 3.14 A, B, C&D and 3.15 A&B all number 1).

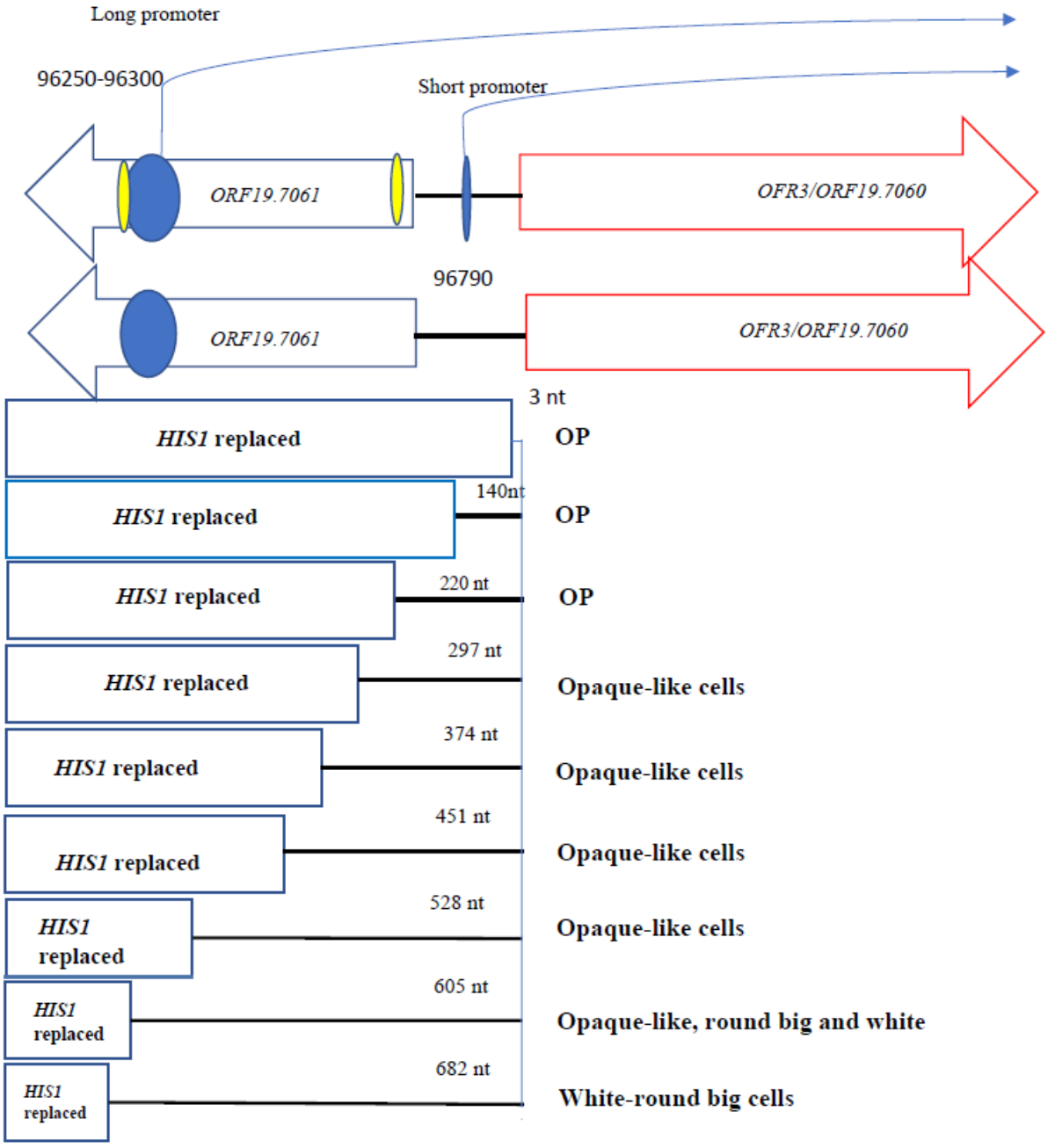

Figure 3.12 Serial heterozygous deletions of the 5'-UTR region of *ORF19.7060* the size of deletion has been made heterozygous into the 5'-UTR of *ORF19.7060* region, the size of DNA region left after each deletion to the start codon of the *ORF19.7060* and the genomic position of long and short promoter and the approximate distance of these

promoters with each deletion. 1) the long(white) transcript TATA box, 2) the short(opaque) transcript TATA box.

MA201 has the largest 5'-UTR of *ORF19.7060* deletion of region, 860 nucleotides in this region were replaced by the *HIS1* marker, 5'-upstream *ORF19.7060-No1+/Δ*, deletion extending from position 96778 to 95918 (Fig.3.4). MA201 colonies were distinguishably switched from white to pink colonies over the SC-GLcNAc plate. These pink colonies displayed the characteristics of opaque cell colonies; they were flattened and distinctively spread over the agar plate. Microscopic observation identified large, elongated opaque-like cells within the pink colonies. I further tested using opaque-specific antibody staining, which showed that the elongated cells were truly opaque since they showed the characteristic antibody staining in immunofluorescence microscopy Fig. 3.13 B. The frequency of the W/OP transition in these cells is shown in table 3.7.

Strain MA202 was second largest in terms of deletion, in 5'-UTR of *ORF19.7060-No2+/Δ*; 706 nucleotides were deleted in this strain; extending from genomic region 96624 to 95918. Similar to MA201, MA202 also generated pink colonies on the SC-GLcNAc plate. These pink colonies were flattened and distinctively spread over the agar plate and also showed classic opaque characteristics. Microscopic observation identified similar opaque-like cells designated pink colonies. To analyze the nature of true "opaque" in these cells, a supplementary examination was performed using opaque-specific antibody staining and immunofluorescence microscopy. These elongated opaque-like cells exhibited true opaque characteristics (Fig.3.13 C). The frequency of the W/OP transition in these cells is shown in Table 3.7

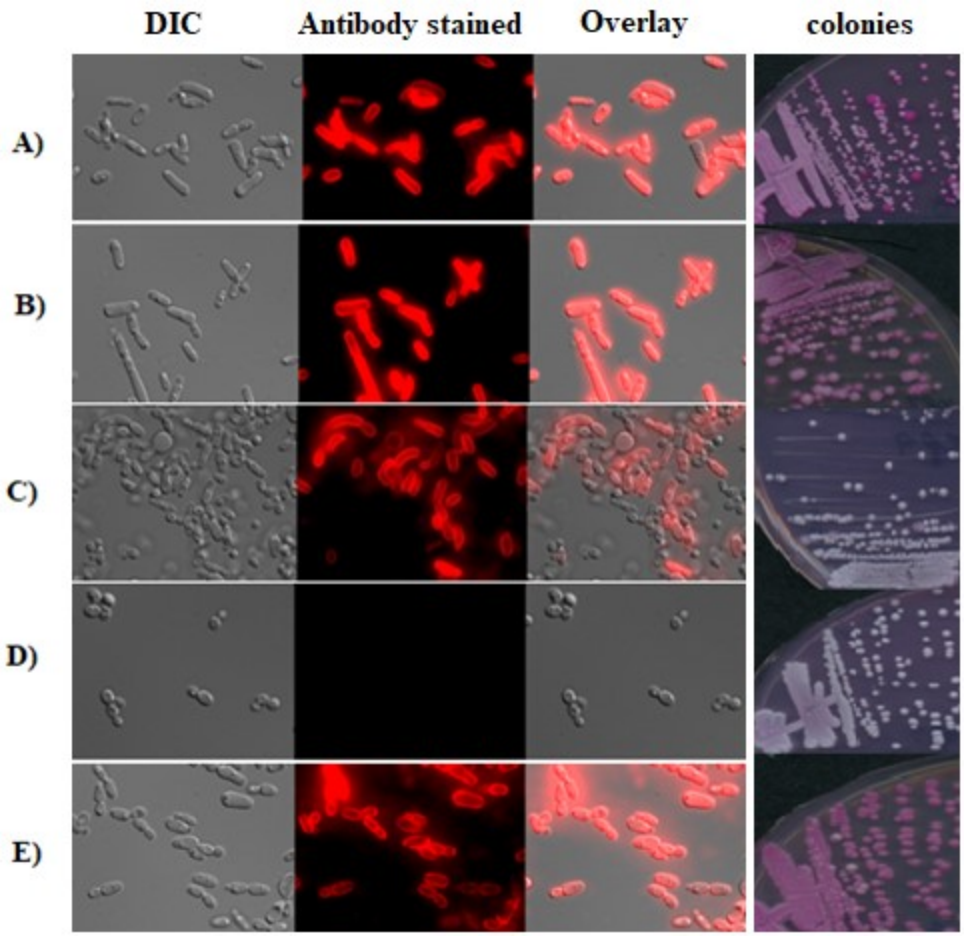

Figure 3.13 Cell and colony characteristics of specified strains. Cells from positive phloxine B staining colonies grown at 25 °C for 4-6 days were assessed microscopically and photographed with a Leica DM6000 fluorescence microscope at 630X magnification. Cells were analyzed for cell morphology (DIC), for staining with the opaque-specific antibody F223-5E1-1 with Texas red conjugated goat anti-mouse antibody as the secondary antibody (Antibody stained), and by overlay of the images (Overlay). The phloxine B staining colonies were also streaked for single colonies on SC-GlcNAc plus phloxine B agar medium (Colonies).

A) Strain MA40 *MTL **a**/α* deletion from genomic region 96928 to 95918 three base pairs (bp) before the start codon of *ORF19.7060,* heterozygously removing the entire 5'-UTR of *ORF19.7060*

B) Strain MA201 *MTL **a**/α* 860 bp of the 5'-UTR of *ORF19.7060* was heterozygously deleted.

C) Strain MA202 *MTL* ***a/α*** 706 bp of the 5'-UTR of *ORF19.7060* was heterozygously deleted.

D) SN76 parental strain *MTL* ***a/α***.

E) The strain3745 **a/a**

Although the deletion (5'-UTR of *ORF19.7060-No3+/Δ*) in strain MA203 was extensive (625 nucleotides, extending from 96543 to 95918 in the *ORF19.7060* promoter region), MA203 did not display the true opaque characteristics in the elongated opaque-like cell. Although MA203 at the colony level exhibited pink, flat colonies, the individual cells did not show the true opaque pattern of staining assessed by immunofluorescence microscopy (Fig.3.14 A). The frequency of this switching is displayed in the Table.3.7.

Strain MA204, 5'-UTR of *ORF19.7060-No4+/Δ* deleted 552 nucleotides of the up-stream region of *ORF19.7060*, extending from the genomic region 96470 to 95918. MA204 also generated distinguishable pink colonies consisting of elongated opaque-like cells that did not display the true opaque staining pattern in immunofluorescence microscopy Fig.3.14 B. The frequency of switching white to pink colonies is shown in (Table 3.7).

The pattern of MA203 and MA204 was repeated in strain MA205. MA205 deleted 475 nucleotides in, 5'-UTR of *ORF19.7060-No5+/Δ* which contained genomic region 96393 to 95918. The same pink colonies were observed on plates; the frequency of this white to pink switching is shown in Table 3.7. All the opaque-like cells in these pink colonies failed to show opaque-specific antibody staining in immunofluorescence microscopy Fig.3.14 C.

Strain MA206, 5'-UTR of *ORF19.7060-No6+/Δ* deleted 398 nucleotides of the *ORF19.7060* up-stream region consisting of the genomic region 96216 to 95918. Pink colonies of MA206 were identified; the frequency is shown in Table 3.7. The pink colonies from this strain contain a mixture of distinctively different cell types including elongated opaque-like cells, large round cells and normal white yeast form, a pattern quite different from the previously mentioned ones. None of these morphologically different cells demonstrated the true opaque staining pattern during the microscopic analysis (Fig.3.14 D).

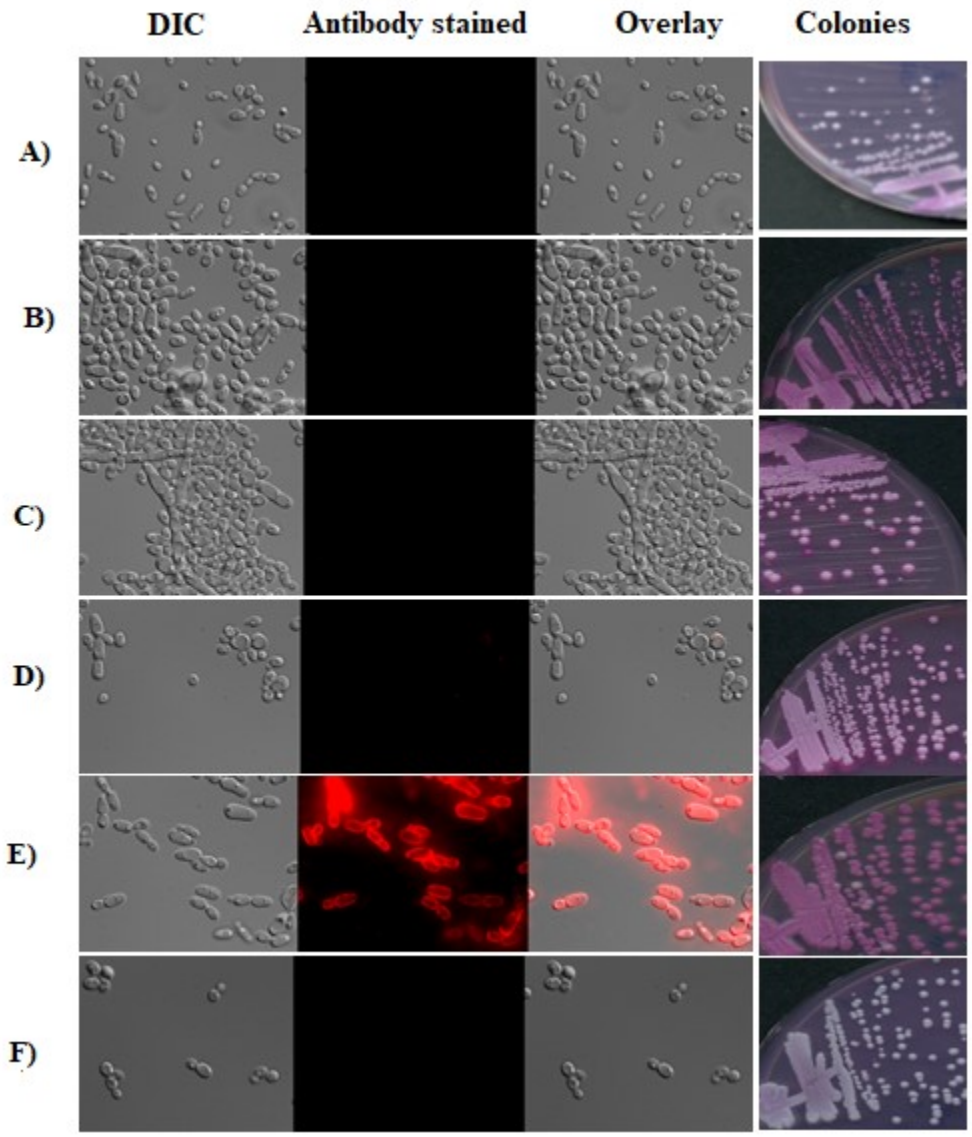

Figure 3.14 Cell and colony characteristics of specified strains. Cells from positive phloxine B staining colonies grown at 25 °C for 4-6 days were assessed microscopically and photographed with a Leica DM6000 fluorescence microscope at 630X magnification. Cells were analyzed for cell morphology (DIC), for staining with the opaque-specific antibody F223-5E1-1 with Texas red conjugated goat anti-mouse antibody as the secondary antibody (Antibody stained), and by overlay of the images (Overlay). The phloxine B staining colonies were also streaked for single colonies on SC-GlcNAc plus phloxine B agar medium (Colonies).

A) Strain MA203 *MTL* ***a/α*** 625 bp of the 5'-UTR of *ORF19.7060* was heterozygously deleted.
B) Strain MA204 *MTL* ***a/α*** 552 bp of the 5'-UTR of *ORF19.7060* was heterozygously deleted.
C) Strain MA205 *MTL* ***a/α*** 475 bp of the 5'-UTR of *ORF19.7060* was heterozygously deleted.
D) Strain MA206 *MTL* ***a/α*** 398 bp of the 5'-UTR of *ORF19.7060* was heterozygously deleted.
E) Strain3745 **a**/**a**
F) SN76 parental *MTL* ***a/α***

Strain MA207; mutant, 5'-UTR of *ORF19.7060-No7+/Δ,* contained a deletion of 321 nucleotides which extended from genomic region 96239 to 95918. In MA207 the pink colonies appeared after 7 days. The frequency of switching from white colonies to pink demonstrated in Table 3.7. The pink colonies were a mixture of cell types including opaque like elongated cells, round big cells and normal white cells that were previously seen in MA206. None of the morphologically different cells stained with the opaque-specific antibody (Fig.3.15 A).

Strain MA208, mutant, 5'-UTR of *ORF19.7060-No8+/Δ* has the smallest deletion in the *ORF19.7060* up-stream region. This deletion replaced the section between genomic region 96162 to 95918 and only removed 244 nucleotides. The pink colonies of MA208 selected for microscopic observation contained mostly normal white cells with a limited number of round big cells (Fig. 3.15 B). The frequency of white-pink colonies shown in Table 3.7.

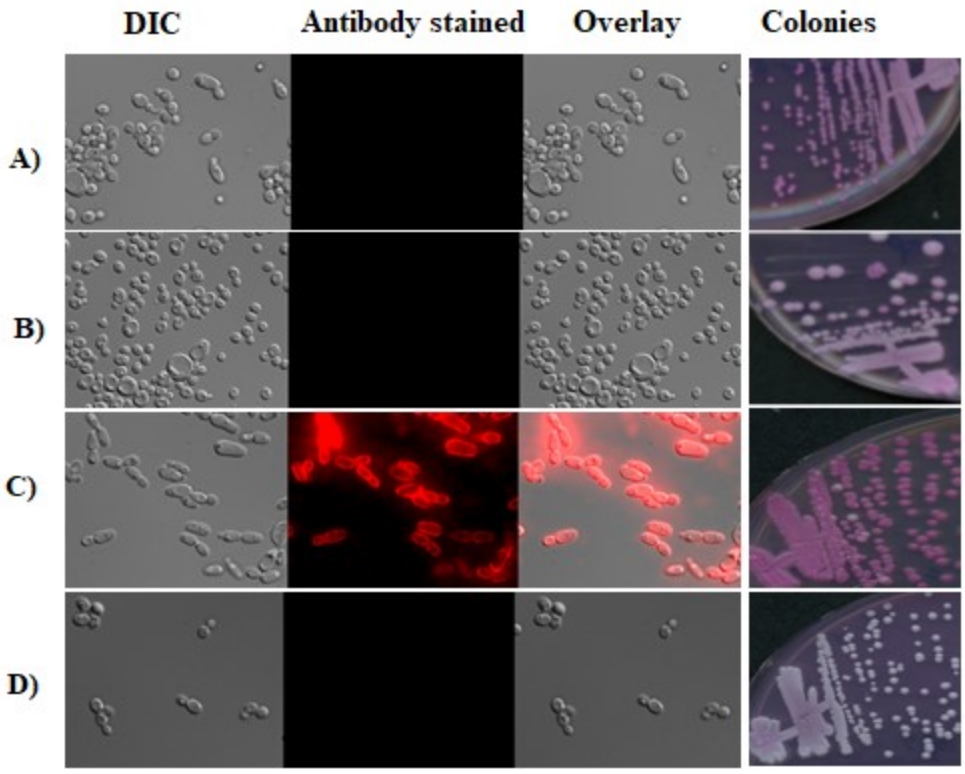

Figure 3.15 Cell and colony characteristics of specified strains. Cells from positive phloxine B staining colonies grown at 25 °C for 4-6 days were assessed microscopically and photographed with a Leica DM6000 fluorescence microscope at 630X magnification. Cells were analyzed for cell morphology (DIC), for staining with the opaque-specific antibody F223-5E1-1 with Texas red conjugated goat anti-mouse antibody as the secondary antibody (Antibody stained), and by overlay of the images (Overlay). The phloxine B staining colonies were also streaked for single colonies on SC-GlcNAc plus phloxine B agar medium (Colonies).

A Strain MA207 *MTL* ***a/α*** 321 bp of the 5'-UTR of *ORF19.7060* was heterozygously deleted.

B) Strain MA208 *MTL* ***a/α*** 244 bp of the 5'-UTR of *ORF19.7060* was heterozygously deleted.

C) Strain 3745 **a**/**a**

D) SN76 parental *MTL* ***a/α***

The results of the sequential deletions from the *ORF19.7060/ORF19.7060* up-stream region can be summarized into three groups. The first two deletions showed the formation of true opaque

cells. In the next group, this morphological pattern shifted to large, elongated opaque-like-cell in the four next mutant strains. Finally, in the last two deletions, this pattern changed mostly to ordinary white cells and a limited number of large, round cells in the pink colonies which suggests a very distinctive role for the 5'-UTR of *ORF19.7060* in preventing the W/OP switching in *MTL* **a**/α strain.

Strain	Total colonies	Pink colonies	Ratio%
SN76	550	0	0%
MA-201	336	5	1.4%
MA-202	398	7	1.7%
MA-203	320	4	1.8%
MA-204	457	6	1.3%
MA-205	454	7	1.53%
MA-206	348	6	1.7%
MA-207	423	6.5	1.5%
MA-208	478	5.5	1.1%

Table 3.7 Rate of white-to-pink switching in the strains MA201-208. The ratio of white to pink switching of all experimental samples were calculated from among 100 to 500 colonies in total after 4-7 days incubation at room temperature. Carbon sources used were GlcNAc (GLC). Strains were all initiated from white (WH) cells. The ratios are based on at least 3 separate experiments.

3.4 Protein structure analysis

The protein structure of Orf19.7060 identified an XLF domain. This domain was initially identified in the Xrcc4-like-factor that interacts with the XRCC4-DNA ligase IV complex to promote DNA nonhomologous end-joining (NHEJ) [79]. It also suggested that *ORF19.7060* is an ortholog of *NEJ1* in *S. cerevisiae. NEJ1* is one of the genes regulated by *MAT*; it is repressed in diploid form *MAT* **a**/α cells after mating [80]. The protein alignment for Orf19.7060 in *C. albicans* and Nej1 in *S. cerevisiae* is shown in Fig.3.16 A. The preserved identical domains and serine/threonine at the

same positions that are potentially phosphorylated are also noted with the oval circle[81, 82]. I also made a comparison between the Orf19.7060 protein and XLF domain in humans since this domain is well studied for nonhomologous end-joining in mammalian cells. The Protein BLAST for Orf19.7060 with the human XLF domain displayed the identified serine/threonine at the same residue preserved in the protein domain as well (Fig.3.16 B) [83]. The comparison between these two alignments also supports the idea about the phosphorylation as a post translational modification in this protein. Studies also suggested that the XLF protein is enriched and phosphorylated at the replication forks of human cells and proposed the CDC7p kinase (a kinase required for DNA synthesis initiation) which could be responsible for XLF phosphorylation. Therefore, it is possible that XLF is one of the key components in NHEJ and also plays a role in stabilizing replication by attaching to double-strand DNA [84].

C. albicans is an obligate diploid [85] and we know that *ORF19.7060* has two different promoters in white (long transcript) and opaque (Short transcript) cells. I performed a Western blot for Orf19.7060 protein in both cell states to detect this protein on both white and opaque cells and also to find and assess whether there are differences in these cell types.

I replaced one allele of *ORF19.7060* in strain SN148 **a**/**a** by *HIS1* and added a TAP protein tag which can be identified by anti-TAP polyclonal antibody to another allele. Then I examined the behaviour of the tagged protein in white and opaque versions of the SN148 **a**/**a** cells. Western blotting shows that the Orf19.7060 (XLF) protein extracted from white cells has a different pattern of migration compared to the protein extracted from opaque cells. The XLF protein in the white cell followed a similar pattern of migration to the XLF protein in humans, showing two distinct migrating bands. In humans, this pattern of migration suggested the active form of the XLF protein was the slower moving phosphorylated protein [79], when it acts as the NHEJ counterpart with Ku proteins and XRCC4 [86, 87]. In contrast to white cells, in opaque cells Orf9.7060-*tap* tagged (XLF) migrated with only one band, which displayed the slower migration pattern (Fig.3.17).

Figure 3.16 NCBI-Protein blast, protein alignment **A)** protein alignment of Orf19.7060 *C. albicans* and Nej1 in *S. cerevisiae*. **B)** protein alignment of Orf19.7060 *C. albicans* and human XLF, the serine/threonine's conserved in the protein domain were highlighted by oval circles[83].

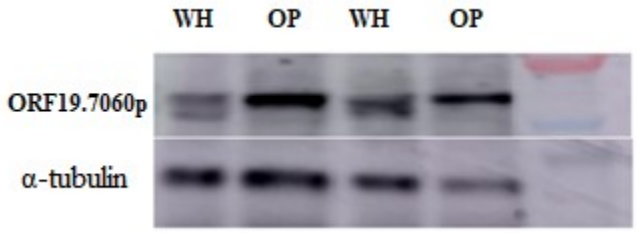

Figure 3.17 The polyacrylamide gel result of western blot from Orf19.7060 protein, which was extracted from the cells in white and opaque state. The slow movement of the protein in opaque state is compatible with the phosphorylated protein (As post translational modification) which is considered to be the active form of this protein in the cells. α-tubulin was used as a protein expression control in this experiment.

3.5 Mating assay

The opaque state is considered to be pre-requisite for the mating in *C. albicans* [12]. Since both MA10 and MA40 displayed the true-opaque pattern of staining in the immunofluorescence microscopy, I performed mating assays to analyze the potential mating ability in both MA10 and MA40. I also searched both transcriptomes to identify expression patterns of genes involved in pheromone response and mating pathways. In this study, both MA40 and MA10 were crossed with both *3315α/α* and *3745* **a**/**a** tester strains. The result demonstrated that MA40 poorly mated with both tester strains, generating a very limited number of colonies on the selective marker plate (Ura and Trp).

The frequency of mating was lowest in MA10, as after two mating assays only one colony appeared each time with either with **a**/**a** or α/α tester strains. The low efficient mating abilities of MA10 and MA40 meant that they should be considered as non-mating strains, and that the mating observed could be due to independent loss of heterozygosity (LOH) at the *MTL* locus [39]. (Fig.3.18 C&D). In addition, none of the hierarchical deleted mutants (MA200-208) went through the mating process with either of **a**/**a** or α/α tester strains (data not shown).

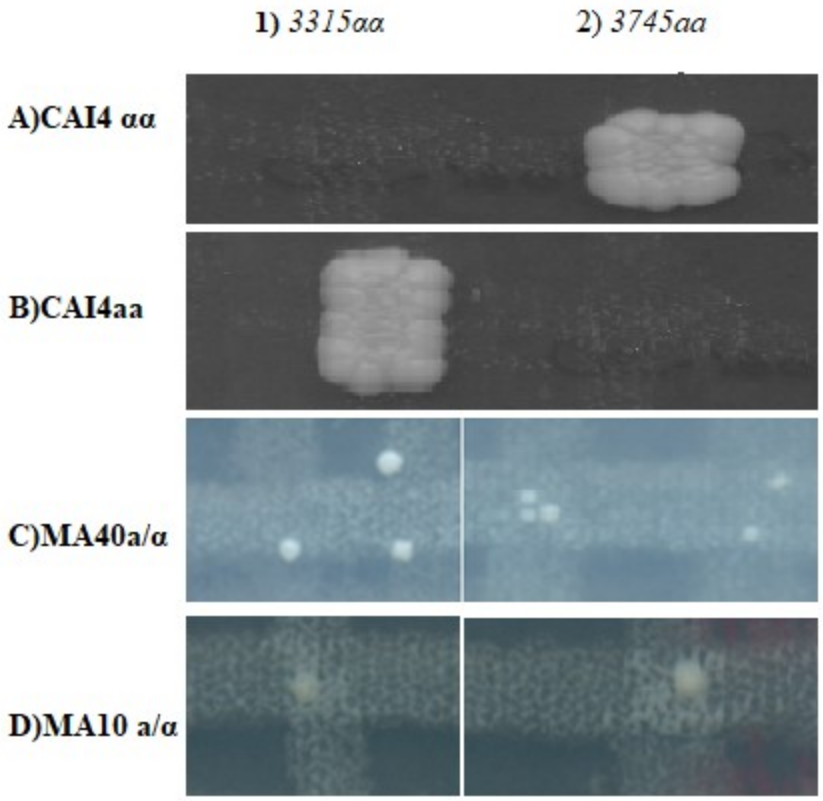

Figure 3.18 A) Mating between CAI4 α and tester strain 3745aa. **B)** Mating between CAI4a and tester strain 3315. **C)** Shows mating between MA40 a/ α and the both tester strain. **D)** Mating between MA10 and both tester strains. MA10 and MA40 undergo mating with both wild type *MTL* homozygous strains in a very low rate compare to the control. Strains 3745 **a/a** and 3315 α/α, in the opaque state, were used as mating type testers. They had the auxotrophic markers *TRP1/TRP1; LYS2/LYS2*. These testers were crossed with MA10 and MA40 (*ARG4/ARG4; URA3/URA3*) on GlcNAc medium at RT for two days and then replicated on selection medium YCB-glucose (Trp-,Ura-) at 30°C for 3 days to detect auxotrophic mating products.

The genes involved in pheromone responses include *STE2* [88, 89], *STE3, STE4, CAG1,* and *STE18*,[90]. The MA10 expression profile showed only *STE4* was expressed with less 1.5-fold changes; however, in the MA40 expression data, all the pheromone response genes were expressed more than 2-fold changes except *STE2* (Table 3.8).

The genes are involved in both MAP kinase and mating pathways such as *CST20, STE11, HST7, CST5*, *CEK1,* and *CPH1*[77, 91]. There is another gene, *CEK2* [91, 92] which has overlapping functions with *CEK1* in the mating pathway [53]. In MA10 data expression, *CEK2* and *CST5* have detectable expressions with more than 2-fold changes while the rest are expressed insignificantly. Similar to MA10, the data expression of MA40 displayed significant expression level for *CST5* and *CEK2* more than 2-fold changes, yet for other genes in this pathway such as *CPH1, CST20, STE11,* and *CEK1* the expression displayed less than 1.5-fold changes. Moreover, negative expression was observed for *HST7*. Table 3.9 illustrated these two pathways expression levels in both MA10 and MA40 transcriptome.

Name	**MA10/fold change**	**MA40/fold change**	**Opaque/fold change**
MFalpha	NO	9.2	12.8
MFA	NO	NO	9.9
STE2	NO	NO	5.7
STE3	NO	8.3	10.9
STE4	1.2	8.1	1.5
CAG1	0.4	4.4	2.4
STE18	0.9	2.2	1.7

Table 3.8 The pheromone response pathway genes expressed in both MA10 and MA40 compared to the true opaque expression for these genes.

Name	MA10/fold change	MA40/fold change	Opaque/fold change
CST20	-0.01	0.9	-0.08
STE11	1.5	0.8	0.7
HST7	0.3	-0.4	1.1
CST5	2.1	2.3	3.1
CPH1	-0.3	0.5	3.7
CEK2	4.5	6.1	6.9
CEK1	0.7	1.2	5.2

Table 3.9 The expression levels of MAP kinase and mating pathway genes in both MA10 and MA40 compared with true opaque gene expression

3.6 Creating double deletion of *ORF19.7060-ORF19.7061*

As mentioned before, both *ORF19.7061* and *ORF19.7060* are quite close in terms of genomic distance, approximately 200 nucleotides. Moreover, *ORF19.7060* long transcript is expanded roughly in 2/3 of *ORF19.7061*, which results in the inevitable deletion of *ORF19.7061* if the complete deletion of *ORF19.7060* for both promoter regions were made. Considering this fact, to have a clear result and to mitigate the risk of any remaining regions both genes were deleted in SN76 **a**/α which enabled us to observe W/OP transition in this strain.

The double deletion strain of *ORF19.7060Δ/Δ-ORF19.7061 Δ/Δ* was created in SN76 **a**/α as a parental strain by replacing the entire region with *ARG4* as a replacement and using CRISPR_CAS9 method for deletion. The null mutation and the *MTL* **a**/α by colony PCR were

confirmed. Further investigation to observe the transition, started by streaking the mutant over the SD-GlcNAc plate and formation of opaque colonies over the plate after 4-6 days. The result showed that the strain switched to opaque and stayed **a**/α for a limited time, but they lost the heterozygosity for the *MTL* locus at the end and went through mating with one of the testers 3315 α/α.

3.7 Secretory aspartyl proteinase (SAP) activities

As previously mentioned, *ORF19.7061* is the adjacent gene to *ORF19.7060* and it is an ortholog to *YHF7 in S. cerevisiae (The Candida Genome Database (CGD).* Based on the information that had been found in SGD (https://www.yeastgenome.org), *YHF7* is one of the putative uridine kinases which contains a P-loop motif that is a common structure in many ATP- and GTP-binding proteins. It is helpful to know that the primary structure of the P-loop motif typically contains a glycine-rich sequence which is followed by a conserved lysine and a serine or threonine [93].

The protein structure and homology of *ORF19.7061* was obtained from the computational tools to analyze the protein structure addressed to the hydrolytic function of the ORF19.7061 protein [94]. To assess the hydrolytic function of this protein, SAP activities were performed. In this study three different control strains were SN76, MA10 (*ORF19.7061* homozygous deletion) and MA40 (*ORF19.7061* heterozygous deletion), The three experimental strains were SN76-CIP-*ORF19.7061*, MA110 (MA10-CIP-*ORF19.7061)* and MA410 (MA40-CIP-*ORF19.7061*). All the *ORF19.7061* PCR constructs were expressed under control of the *ACT1* promoter and inserted in RP10 genomic region. The result demonstrated that all the strains that expressed the *ORF19.7061* PCR construct under the *ACT1* promoter elevated the SAP activity and created a halo on the YCB-BSA plate. Fig.3.19 A, B & C. Recently stated outcome in addition to the result that achieved from complementation and gaining sensitivity for CFW (Calcofluor-white) can be considered as a milestone for further experiments and studies about the real function of this ORF in *C. albicans* [25]. The size of halo was measured and exhibited in (Table 3.10).

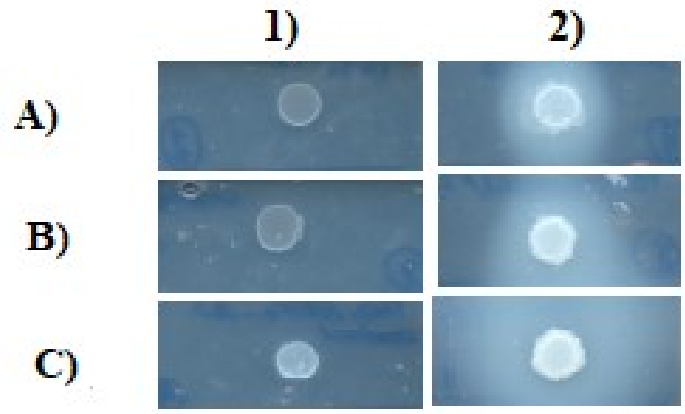

Figure 3.19 A1) SN76 parental strain, **A2)** SN76 plus *ORF19.7061* under the *ACT1* promoter. **B1)** MA10 and B2) MA110(MA10 plus *ORF19.7061* driven by *ACT1* promoter. **C1)** MA40 and **C2)** strain MA410 plus *ORF19.7061* driven by *ACT1* promoter. Each sample 5 µl spotted on YCB-BSA plate and kept at 30˚C for 7 days. The halo formed only around the strains that contain *ORF19.7061* driven by the *ACT1* promoter.

Strain	Halo size
SN76	NO
MA10	NO
MA40	NO
SN76 CIP*ORF19.7061*	3.83 mm
MA110 (MA10-CIP*ORF19.7061)*	6.5 mm
MA410 (MA40-CIP*ORF19.7061)*	11.66 mm

Table 3.10 Size of halo created on YCB-BSA plate after the insertion of *ORF19.7061* driven by *ACT1* promoter in the strain SN76 parental strain, MA10 and MA40.

3.8 Assessing the effect of ectopic expression of both long and short *ORF19.7060* transcripts on white-opaque switching in the *MTL* homozygous strain background

Because deletion of *ORF19.7060* was permissive for the W/OP transition in the SN76 **a**/α background strain, I investigated whether the expression of this gene could have an effect on the rate of W/OP switching. To address this question, I determined the effect of ectopic expression of this gene on *MTL* homogygous strains with a normal ability to transition from white to opaque. Previous studies showed a change in the promoter region of white and opaque state cells; the transcript expressed in white cells was longer than the transcript in opaque state cells [74]. This longer transcript in white cells was called the "long transcript", while that in opaque cells was designated the "short transcript". We also evaluated the effect of ectopic expression of the long and short transcripts of *ORF19.7060* in strain CAI4 **a**/**a**.

In this experiment, I designed two different PCR products. The DNAs encoding the long and short transcripts of *ORF19.7060* were amplified and ligated under control of the *ACT1* promoter in plasmid CIP. Subsequently, plasmids containing either the long or the short transcript driven by the *ACT1* promoter were independently transformed into strain CAI4 (*MTL* **a**/**a**). The results showed an approximate doubling in W/OP switching was observed in the *MTL* homozygous CAI4 background strains as a result of the ectopic expression of either the long or the short transcript of *ORF19.7060* when compared with the wild type (Table 3.11). Thus, neither long nor short *ORF19.7060* transcripts appear to have a strong effect on the W/OP switching in this *MTL* **a**/**a** strain.

Strain	Total colonies	Opaque colonies	Ratio%
CAI4**a/a**	8286	125	1.52%
CAI4+*ORF19.7060* long **a/a**	7030	286	4.1%
CAI4+*ORF19.7060* short **a/a**	8980	281	3.5%

Table 3.11 Comparison between the strain CAI4 and CAI4 with the insertion of the long or the short transcript of *ORF19.7060* in creating opaque phenotype colonies on SC-GLcNAc plates after 6 days.

DISCUSSION

Candida albicans cells exist in many morphological states [95]. Two well established morphologies are the white and opaque forms, and these forms flip from one to the other under the control of a master regulatory transcription factor called *WOR1* (White Opaque Regulator1) [54, 60]. High levels of *WOR1* generate the opaque state program by activating a large number of opaque specific genes, including *WOR1* itself [14]. This positive loop results in a stable epigenetic opaque state; disruption of the loop switches the cells into the low *WOR1* white state [96].

Cell that are heterozygous at the mating type like (*MTL*) locus cannot switch to the opaque state because *MTL* encodes a heteromeric repressor protein, made up of the **a**1 and α2 proteins, that blocks *WOR1* expression [76]. Because expression of *WOR1* and establishment of the opaque state is critical for cells to become mating competent, typical *MTL* **a**/α *C. albicans* cells are non-mating [97]. Switching to the opaque, mating competent state is normally limited to cells that have become homozygous at *MTL*, and thus no longer make the **a**1-α2 repressor [30]. However, some conditions have been identified that allow de-repression of the W/OP transition in cells that are heterozygous *MTL* ***a***/α. For example, deletion of *OFR1*, which encodes a Yci domain protein, allows W/OP switching and mating in *MTL* ***a***/α heterozygotes [62]. Heterozygotes of the essential *HBR1* locus, which encodes a hemoglobin binding protein, allowed opaque phase switching and mating, and reduced the expression of *MTLalpha*1 and *alpha*2 [98]. As well, deletion of specific transcription factors such as *EFG1,* the white specific transcription factor [99]*, BRG1,* a transcription factor that is required for hyphal formation [100] and *RFG1,* a transcription factor required for filamentous growth and biofilm formation [101], separately allow the cells to switch into the opaque state while the cells are *MTL* **a**/α [76]. Deletion of another transcription factor, *SFL2*, de-represses the opaque phenotype in *MTL* **a**/α cells in a carbon source dependent manner (GLcNAc as an inducer and Glucose as a suppressor) at physiological temperatures (37˚C) and high CO2 (5%) [102].

I have investigated another locus that influences the W/OP switching process. Cells that lack or are heterozygous for a region upstream of *ORF19.7060* are able to switch to the opaque state even when heterozygous at *MTL*.

RNAseq analysis of strain MA10, where both alleles lack this 5'-UTR of *ORF19.7060*, showed that both the *MTL**a*** and *MTLalpha* genes were expressed in this strain; this result was consistent with the result of *MTL* colony PCR and sequencing for *MTL**a**2* and *MTLalpha1,* which showed

both regions were present in the genome. In spite of the expression of the genes encoding the **a**1-α2 repressor, *WOR1* was expressed as highly in MA10 as in the transcriptome of true opaque cells. This strain also showed the expression of *WOR4* [59] to be slightly higher than in the true opaque data set. MA10 also expressed other genes involved in opaque circuitry such as *WOR3, OP4, CZF1, PHO89* and *PHO8,* this strain also down-regulated the white specific genes that normally derepress in classic opaque cells the genes such as *WH11, AHR1* and *SSN6* (Table 3.3) [103]. However, MA10 did not express all the genes up-regulated in true opaque cells generated from *MTL* homozygous strains; the genes differentially transcribed in MA10 compared to the classic opaque transcriptome can be divided into two different groups.

The first group, the genes are not up regulated in the MA10 transcriptome but are up-regulated in the standard opaque data – part of this set consists of the genes that are regulated by *EFG1.* A key gene in this set is *WOR2*, encoding a transcription factor required for the maintenance of the opaque phenotype [51]. Other genes in this group regulated by *EFG1* play roles in hyphael formation and virulence, such as *HWP1,* encoding a hyphal cell wall protein which is highly expressed on the opaque cell surface during mating [104]; this gene is placed downstream of *EFG1* in the hyphal formation pathway [105]. *HWP1* was dramatically down-regulated in the MA10 transcriptome. *RBT1* is another gene in this group; this gene is similar to *HWP1* as it encodes a cell wall protein, and the full expression of this gene is dependent on *EFG1* expression [106]. MA10 also down-regulated *ALS1* more than was observed in the classic opaque data set; this gene also plays a role in virulence and acts downstream of *EFG1* [107] in this pattern of expression it assumed that *EFG1* is the suppressor in a classic opaque cells then when the *EFG1* goes down these genes will go up, but suprizingly *EFG1* in MA10 did not go down as classic opaque cell in the normal situation then these genes down-regulated in MA10 subsiquently (Table 3.4).

Another set of the genes not highly expressed in MA10 that are up-regulated in classic opaque cells are those involved in cell type in *C. albicans*. In the MA10 RNA seq data, **a** and α-specific genes were not up-regulated as they are in homozygous *MTL* opaque cells. The **a**-specific genes such as *MF**a**,* encoding the a-factor precursor [108], *STE2,* encoding the α-factor receptor expressed in **a**-cells [109], *SAP30,* the gene for an aspartyl proteinase that plays a role in α-factor degradation [110] and *RHR2* [69] were all less expressed when compared with the classic opaque

data set. MA10 also did not express the α-specific genes, failing to up-regulate genes such as *MFα,* encoding the precursor for α-factor [111] and *STE3,* the gene for the receptor for **a**-factor [38](Fig 3.11 & Table 3.3). These genes normally are up-regulated in opaque cells in a cell-type dependent manner, the **a**-specific genes in *MTL***a/a** cells, the alpha-specific genes in *MTL*α/α cells failed to express.

In the second group are MA10 up-regulated genes that are down-regulated in classic opaque data set. This group can be divided into two sub-divisions. One includes genes that are repressed by α-factor in spider medium MA10 the genes such as *CTF5* (acts in minichromosome maintenance [112]) and *KIP2* (the gene that encode for the kinesin-related motor protein involved in mitotic spindle positioning [113]) were up-regulated. Another co-regulated gene set includes genes that are regulated by the CAP-HAP complex [114]. Genes such as *UCF1* (this gene is induced by high iron and by cAMP during filamentous growth [115]), *PSA2* (encodes Mannose-1-phosphate guanyltransferase, and is repressed by macrophage [116]), *PGA26* (encoding an adhesin-like GPI-anchored cell wall protein with a role in cell wall integrity; this gene is also induced by high iron [117]), *PLB4.5* (encodes Phospholipase B; regulated by *HOG1* and *SSN6*; putative GPI-anchor [117]) and *PGK1* (encodes Phosphoglycerate kinase; repressed upon phagocytosis [118]). All these genes were highly overexpressed compared to control white SN76 **a**/α strain and the classic opaque data sets (Table 3.5). The up-regulation of these two groups may be correlated with the presence of a1-α2 in MA10 which blocks the upstream suppressor in their pathway, and due to this suppression these genes express even when the cells switch to opaque.

Because mutation of transcription factors such as *EFG1*, *RFG1* and *SFL2* can create an opaque non-mating phenotype in **a**/α cells [61], the expression of these transcription factors was specifically investigated in the MA10 transcriptome. The result showed that *EFG1* was not down-regulated as in the classic opaque data set. In the normal white condition *EFG1* down-regulates *WOR1* and *WOR2*, and this situation is inverted when the cells switch to opaque, because in the classic opaque circuitry *EFG1* is down-regulated by *WOR1* and *CZF1* [29, 119]. However, *EFG1* was not down-regulated in MA10 as it was in classic opaque cells, although some genes downstream of *EFG1* which are normally expressed in the hyphal condition did not express either,

perhaps suggesting a dual regulatory role for *EFG1* which is correlated to the cell state of white or opaque.

By contrast, *BRG1* was down-regulated as in classic opaque cells, and *RFG1* was down regulated about two fold. The last transcription factor is *SFL2;* this gene is dramatically supressed compared to the classic opaque data set (Table 3.6). In this regard *SFL2* could potentially play a key role in generation of the opaque phenotype in the strain MA10. *SFL2* disruption is permissive for opaque switching in a carbon-source-dependent manner (GLcNAc), 5% CO2 and at 37˚C, and the null mutant of *SFL2* does not mate. The *SLF2* null mutant can switch to opaque at a low frequency (About 0.1±0.2) only when the cells grow on GLcNAc at room temperature [102]. In the MA10 RNA seq result *SFL2* was down regulated about five-fold less than its expression in true opaque data sets, and MA10 does not mate either. However the opaque phenotype created in MA10 due to deletion of both copies of the 5'-UTR of *ORF19.7060* is stable at 25˚C room temperature with the frequency 0.9%, It is possible the stability of the opaque cell in room temperature may be compensated by the over expression of *WOR3,* which is slightly more highly expressed than in true opaque cells and is responsible for the stability of the opaque phenotype at 25˚C [120].

I also generated a heterozygous mutant of the same sequence of the region upstream of *ORF19.7060* to create strain MA40; in strain MA40, only one copy of the 5'-UTR region of *ORF19.7060* was deleted. MA40 has phenotypic similarities to MA10, as well as differences (Table 3.3- 3.5 &3.6). The MA40 transcriptome showed detectable expression of *MTL**a*** and *alpha*, however in this strain the genes at the *MTLalpha* allele had significantly more expression compared to the *MTL**a*** allele. MA40 highly expressed the *WOR1* opaque master regulator and other opaque-specific genes similarly to MA10. MA40 also differentially regulated the genes that are regulated by *EFG1*, with MA40 also up-regulating similar genes to MA10 differentially compared to true opaque data expression (Table 3.5). However, compared to MA10, which showed no cell-type tendency, the heterozygous MA40 strain showed an expression pattern similar to the α-cell type. Genes such as *MTL alpha1*, *STE3* and *MFalpha* are the main genes normally uniquely expressed in an α-type opaque cell. It is possible in this strain the imbalance of expression at the *MTL* locus allowed *MTLalpha1* to escape from the **a**1-α2 repression and subsequently allowed expression of *MFalpha* and *STE3*.

I also investigated the four specific transcription factors whose independent disruptions in an **a**/α strain could de-repress opaque switching. In the MA40 transcriptome *EFG1* was down- regulated similarly to the pattern in the classic opaque data set, while *BRG1*and *RFG1* were down- regulated less than in the classic opaque transcriptome (Table 3.6). *SFL2* also may play a role in MA40 in generating the opaque phenotype, as it is down-regulated more than 2.5 fold. As in MA10, the stability of the opaque phenotype in this strain at room temperature may be aided by *WOR3* over expression. MA40 did not efficiently mate with either **a/a** or α/α tester strains despite the expression of alpha-like cell type genes; this failure was similar to that of MA10 and the *SFL2* mutant strain (Fig 3.18 & Table 3.6).

These results of the gene expression patterns in both MA10 and MA40 (the homozygous and heterozygous mutants for the 5'-UTR region of *ORF19.7060* respectively) raise the question of why disruption of this region can create this specific opaque phenotype in **a**/α cells? *C. albicans ORF19.7060* exhibits different 5' UTRs in white and opaque cells, in this case a long transcript is expressed in white state cells and a short transcript is expressed in opaque phase cells. This indicates the use of alternative promoters specific for the distinct cell types, and thus potentially the different non-coding RNAs may have regulatory roles in W/OP switching and in maintaining these distinct cell types in *C. albicans*. [74]. A significant challenge here is to suggest how modifications in this differentially expressed region in the 5' UTR of *ORF19.7060* can allow for opaque switching in an **a**/α strains.

There are different possible scenarios to address this behaviour. The different 5' UTRs, in particular the longer one, could act in different ways to regulate epigenetic events in the cells. The long 5' UTRs could form a stable secondary structure for mRNA and this may inhibit ribosome scannning and/or accessibility or promote RNA decay, all processed that reduce the translational activity driven by the mRNA [121]. Since we know the *ORF19.7060* long transcript is expressed exclusively in white state cells, this behaviour may hamper the translation of this gene in this cell phase. Any interuption in the 5' UTR of this gene may interrupt the transcription machinery and may affect the expression of this protein in a dose-dependent manner. It is possible the expression of this protein may go up when the secondary structure is interupted and potentially down-regulate transcription factors such as *EFG1*, *BRG1* and *SFL2* and create the opaque phenotype in **a**/α strain.

A dose-dependent scenario may explain why the hererozygous deletion of 5' UTR region of *ORF19.7060* generates the opaque phenotype, but it cannot explain why the overexpression of the long transcript of *ORF19.7060* driven by *ACT1* promoter at the *RP10* region does not complement the wild type phenotype and block switching to the opaque state. It was also possible that it was not the coding sequences per se or simple protein expression within the *ORF19.7060/ORF19.7061* region that was critical for creating the opaque phenotype, rather, it was the change in the genomic context that allowed de-repression of W/OP switching.

Another scenario to explain the apparent trans-acting function of a non-translated regulatory region of a gene could be RNA-silencing pathways, which may potentially explain the site-specific phenotype and activity of the heterozygous mutant. RNA-silencing pathway may modulate the mRNAs with different processes such as those that contribute to transposon silencing, viral defense, DNA elimination, heterochromatin formation, and posttranscriptional repression of cellular genes [122, 123]. RNA interference (RNAi) is the simplest explanation in this case as it acts to repress cellular genes through post-transcriptional repression. For many years RNAi has been presumed lost in all budding yeasts. Both the Dicer and Argonaute genes that play the main role in the RNAi pathway are absent in *S. cerevisiae,* but both have an enigmatic presence in *C. albicans* [124]. In the RNAi pathway, the Dicer protein uses a double stranded RNA (dsRNAs) template created by bidirectional transcription to generate small (20-30 nucleotide) interfereing RNAs (siRNAs); these RNAs play roles as a guides and form a complex with Argonate (AGO) and create the RNA-Induced Silencing Complex (RISC). The AGO protein contains two domains, designated the PAZ and PIWI domains. The PIWI domain has nuclease activity and can cleave targated RNA transcripts. In addition RISC can modifiy chromatin structure and block protein synthesis leading to gene repression [123]. The bidirectional transcript of the guide RNAs in the RNAi pathway may explain the site-specific 5' UTR region of *ORF19.7060* which was not complemented by the insertion of one copy in the *RP10* region, and it also may explain in this way that it has the different overlapping regions since the intruption in this region heterozygously can create the opaque phenotype. The 5' UTR region of *ORF19.7060* may play a role as a template for silencing elements of the white-opaque transition machinery. Since *WOR1* positively regulates W/OP switching in an all-or-none pattern [52] then when the inhibition of this silencing pathway disappears then it can express and get raise and start the opaque circuitry in both MA10 and MA40 **a**/α strains

Another explanation can be in the way that an siRNA template from this region guides the RISC complex to the different targets; these different targets may have an inhibitory effect on the "unknown target" that supresses the the expression of transcription factors such as *EFG1, BRG1* and *SFL2* in normal conditions. While this pathway works and this suppression element hamperd, then the transcription factors express and cell stays in the white state. Interuption of the 5' UTR region of *ORF19.7060* (the guide RNA region) releases the suppression element and down-regulates the transcription factors, subsequently the *WOR1* and *WOR4* are released from the repression of the transcription factors such as *EFG1* and overexpress to start the opaque circuitry. This opaque phenotype created by the both strain MA10 and MA40 may not be the prerequisite opaque phenotype for mating in *C. albicans*, it may be a strategy to decrease the virulence and escape from PMNs phagocytosis, since most hyphal-specific genes such as *HWP1, ALS1* and *RFG1* were down- regulated in both strains. The RNAi pathway for post-transcriptional gene silencing (PTGS) has not yet observed in *C. albicans* [124] but the new gene regulatory system may affect indirectly the regulation of virulence genes through the impact on morphological switching.

4.2 Protein structure analysis

ORF19.7060 has unique architecture. In the white state, the long transcript of *ORF19.7060* starts in genomic position 96250-96300 and in the opaque phase, the short transcript starts in the genomic position ~96790. My investigation of the *ORF19.7060* structure identified an XLF domain [125]. The best ortholog of this gene with the XLF domain in yeast (Fig.3.16 A), is required for efficient NHEJ (Non-Homologous-End-Joining) [80]. In *S. cerevisiae* NHEJ is turned off by the **a**1-α2 repressor in the diploid form because of the efficiency of HR (homologous recombination), and perhaps to prevent the danger that may be caused by NHEJ during meiosis [33]. In humans XLFp is Xrcc4-like-factor which interacts with the XRCC4-DNA ligase IV complex to promote nonhomologous end-joining of DNA [79]. Protein BLAST for Orf19.7060 with *NEJ1* in *S. cerevisiae* and the human XLF domain displayed conserved serine/threonine residue preserved in all t three protein domains. Studies suggested that phosphorylation of these serine and threonine residues may activate this protein domain [83, 126] (Fig.3.16 B). This result was interesting enough to encourage me to investigate Western blot experiments. The Western blot investigation identified distinct patterns of migration, suggesting a possible post-translational modification of

Orf19.7060p in the opaque state due to the slower migration of the protein in the gel (Fig.3.17). The translated protein of *ORF19.7060* in the opaque phase that only moved with one slower band suggested that this form of protein underwent post-translational modification. However, the white state pattern of movement showed two bands that were comperable with the form of XLF protein in humans (mentioned in refence 80) and considered to be partially phosphorylated as a post-translational modification (Fig.3.17). This conclusion actually rejected our primary hypothesis about the complete active form of the protein would have been express in white state cells. If this conclusion is true, then the phosphorylated form of protein was expressed in opaque form cells then it can be considered an active form of XLF protein due to the studies before [79]. These results plus the fact about two different promoter regions in white and opaque state may suggest two different roles for this protein in these two different cell phases. It may be that this protein has a role in nonhomologus end joining in one cell phase and acts as a complimentary partner in replication forks in the other cell state [82]. It may explain the phosphorylation in opaque phase compared to partially phosphorylation of the protein in white state cells. The research also claimed that the enrichment of the XLF protein at the replication fork has happened and this protein was phosphorylated by CDC7 p (Kinase required for DNA synthesis initiation). The research also suggested that *XLF* not only is one of the key components in non-homologous end joining NHEJ but also can play a significant role in keeping the replication fork stable by attaching it to the double-strand DNA [84].

4.3 Mating result analysis

Studies showed that the opaque phenotype created in a/α strains due to the intruption in the specific transcription factors, *EFG1, BRG1, RFG1* and *SFL2* was not a prerequisite for mating, as these null mutant strain were unable to mate with **a/a** or α/α tester strains [61, 102]. It is possible the down regulation of *SFL2* in MA10 and MA40 (respectively 5 fold and 3 fold down regulation compared to the classical opaque data set) is responsible for generating the opaque phenotype in my both strains, so I decided to analysis the pheromone respons and mating pathway genes in both strains and investigate their mating ability with both tester strains.

According to the opaque transcriptome, the genes up-regulated in the classic opaque data expression totalled 237 [38], so in my expression data approximately 53% of the classic opaque specific genes were similarly up regulated (Table 3.3). Since the opaque expression profile has

overlap with the pheromone response and mating pathway, as mentioned before, I searched my data sets for the expression of pheromone response genes, such as *STE2, STE3, STE4, CAG1, STE18;* in addition to MAP kinase and mating pathway genes such as *CST20, STE11, HST7, CST5*, *CEK1*, *CPH1*, *CEK2* and *CEK1* [77, 127]. Based on my analysis, in a group of pheromone response genes in the MA10 expression profile, only *STE4* was expressed, but the expression was not statistically significant due to the cut-off of 1.5-fold changes (Table 3.8). In contrast, in the MA40 expression data, all the pheromone response genes were expressed more than 2-fold differently except *STE2* and *MF**a*** which did not show detectable expression (Table 3.8).

My analysis of the genes which were involved in the MAP kinase and mating pathway was also informative. In the MA10 expression data, *CEK2* and *CST5* showed an over-expression more than 2-fold, *CST20* and *CPH1* were negatively regulated and the expression level of the rest was not statistically significant (Table 3.9). Noticeably, the expression of MA40 displayed visible variation in terms of statistically significant expression levels. In this strain, significant expression level for *CST5 and CEK2* showed more than 2-fold changes, the same as MA10, for *CST20, STE11, CPH1* and *CEK1* the expressions were less than 1.5-fold changes, the negative expression for *HST7* was observed. All expressions level less than 1.5-fold changes in this experiment were considered insignificant (Table 3.9).

Since both strains MA10 and MA40 were heterozygous at the *MTL* locus then the overexpression of *MFα*, *STE3* in MA40 due to the imbalance in the expression of *MTL**a1*** and *MTLα2* caused the expression of *MTLalpha1* so the strain MA40 tends more to be α-type cells (Fig.3.11 &Table 3.3). However this imbalance expression of ***a1*** and *α2* did not save the mating ability in this strain. The result of mating assay showed a low mting rate in both MA10 and MA40. Therefore, I came to the conclusion that the low rate of mating with both testers strains 3315α/α and 3745 **a**/**a** could happen because of the individual cells LOH (Fig.3.18) [53]. This conclusion is consistent with non-mating *SLF2* mutant strain in previous study [102].

4.4 Serial deletion in 5'UTR of *ORF19.7060* create novel results

We assumed that the interuption of the 5' UTR region of *ORF19.7060* as a template for dsRNAs may affect the process of siRNAs (small interferering RNAs) construction in the RNAi pathway. Since intruption into the 5' UTR region of *ORF19.7060,* has an haplo-insufficent impact on derepression of W/OP switching and supresses the transcription factors such as *SFL2* and *RFG1,*

and naturalizes the supressen effect of **a**1-α2 in MA40. So I concluded that the interuption of the 5' UTR region of *ORF19.7060* may have the different overlapping regions since the intruption in this region heterozygously created a global change in the genes expression. Thust I decided to investigate this hypothesis by making a serial deletion heterozygously in to the 5' UTR region of *ORF19.7060,* and study the phenotypes which may create due to the intruption of each possible siRNA template in this region.

My investigation showed that the 5' UTR region of *ORF19.7060,* when I deleted about 700 nucleotides of the region still has an impact on W/OP switching global gene expression and created the opaque phenotype (Fig 3.13). Further intruption in this region by creating the shorter deletion into 5' UTR region may disrupt less dsRNAs construct as a pre-siRNAs teplate and only affected the genes that are capable of altering the morphological shape but inable to express the opaque specific epitope on the cells surface . these strains from MA203 to MA206 created the opaque like phnotype(Fig 3.14). It seems dsRNAs template the region less than 700 nucleotides has an impact on blocking the genes that are responsible for the morphological changes in the opaque pathway. the W/OP switching as an epigenetic event, alter the global gene expression the genes may have role in methabolic pathway , or the one that only responsible for the cell wall permeability in c.albicans. Since the futher disruption of the region created the pinkish colonies over the plate, I assumed that the region that I tampered may contain the template for the siRNAs that block the genes may increase the permeability of the cell wall in the opaque state cells then deletion of this region may cause an increase in the permeability and absorbe the Phloxin-B on the GLcNAc plate. The genes like *RBR1, RHD3,IFF6* and *PGA28* are the cell wall specific genes that up regulated in classic opaque data set need to be investigate in future studies. However these pinkish colonies in the small deletion strain MA207 and MA208 contained a mixture of cells mostly white, big round cells and scattered opaque like cells (Fig 3.15). Therefore, the further investigation may seem to be needed to investigate the hypothesis I made in this chapter and it may have a great impact on our understanding about the opaque circuitry and regulatory elements that controls this spontaneous and epigenetic event in *C. albicans*.

4.5 Future work

There are several promising lines for future investigation. We should investigate the expression profiles of the distinct phenotypes found during this study. For instance, establish the expression

profiles of cells with the opaque-like phenotypes found during the sequential deletions. I think it can also add value to analyze the correlation between the effect of these regions' deletion with the classic opaque circuitry. For example, investigation of the similarity and differences between the classic opaque gene expression profile with our opaque like gene expression profile.

The current study focussed on the effect of deletion in the *ORF19.7060* promoter region on stimulating the W/OP transition in an a/α strain. However, the result of SAP activation generated by the ectopic expression of *ORF19.7061* can be an interesting subject for the future research. I think further research can focus on the detailed characterization of this gene, finding its function and order in the SAP pathway. I think the information that I provided may assist such further studies. It may be interesting to pay attention to different sizes of halo associated with the hydrolytic activity of ectopic expression of this gene over the YCB-BSA which may suggest a relation between the hydrolytic activity and formation of the opaque state. For example, MA10 and MA40 **a**/α can switch to opaque, but the SN76 is unable to switch. The bigger size of halo around MA10 & MA40 strains may have a correlation to the transition of the white cells to opaque cells at room temperature in both strains.

In future, I would be enthusiastic do more research not only about the above-mentioned subjects but also about the transcription profile of the serial deletions; specifically, morphological change in strain MA203 - MA207 to compare in detail the reason behind difference of these strains with MA10 and MA40 *MTL* **a**/α and with the true opaque expression profile.

REFERENCES

1. Wilson, D., et al., *Distinct roles of Candida albicans-specific genes in host-pathogen interactions.* Eukaryotic cell, 2014. **13**(8): p. 977-989.
2. Pérez, J.C., C.A. Kumamoto, and A.D. Johnson, *Candida albicans commensalism and pathogenicity are intertwined traits directed by a tightly knit transcriptional regulatory circuit.* PLoS biology, 2013. **11**(3): p. e1001510-e1001510.
3. Dupont, P., *Candida albicans, the opportunist. A cellular and molecular perspective.* Journal of the American Podiatric Medical Association, 1995. **85**(2): p. 104-115.
4. Sobel, J.D., *Vulvovaginal candidosis.* Lancet, 2007. **369**(9577): p. 1961-71.
5. Zeng, X., et al., *Risk Factors of Vulvovaginal Candidiasis among Women of Reproductive Age in Xi'an: A Cross-Sectional Study.* BioMed research international, 2018. **2018**: p. 9703754-9703754.
6. Pfaller, M.A. and D.J. Diekema, *Epidemiology of invasive candidiasis: a persistent public health problem.* Clinical microbiology reviews, 2007. **20**(1): p. 133-163.
7. Romero Romero, M.L., et al., *Simple yet functional phosphate-loop proteins.* Proceedings of the National Academy of Sciences of the United States of America, 2018. **115**(51): p. E11943-E11950.
8. Vincent, J.L., et al., *Epidemiology, diagnosis and treatment of systemic Candida infection in surgical patients under intensive care.* Intensive Care Medicine, 1998. **24**(3): p. 206-216.
9. Hiller, E., et al., *Adaptation, adhesion and invasion during interaction of Candida albicans with the host--focus on the function of cell wall proteins.* Int J Med Microbiol, 2011. **301**(5): p. 384-9.
10. Mitchell, A.P., *Dimorphism and virulence in Candida albicans.* Curr Opin Microbiol, 1998. **1**(6): p. 687-92.
11. Noble, S.M., B.A. Gianetti, and J.N. Witchley, *Candida albicans cell-type switching and functional plasticity in the mammalian host.* Nature reviews. Microbiology, 2017. **15**(2): p. 96-108.
12. Chandra, J., et al., *Biofilm formation by the fungal pathogen Candida albicans: development, architecture, and drug resistance.* Journal of bacteriology, 2001. **183**(18): p. 5385-5394.
13. Biswas, S., P. Van Dijck, and A. Datta, *Environmental sensing and signal transduction pathways regulating morphopathogenic determinants of Candida albicans.* Microbiology and molecular biology reviews : MMBR, 2007. **71**(2): p. 348-376.
14. Lohse, M.B. and A.D. Johnson, *White-opaque switching in Candida albicans.* Current opinion in microbiology, 2009. **12**(6): p. 650-654.
15. Slutsky, B., et al., *"White-opaque transition": a second high-frequency switching system in Candida albicans.* Journal of bacteriology, 1987. **169**(1): p. 189-197.
16. Hernday, A.D., et al., *Structure of the transcriptional network controlling white-opaque switching in Candida albicans.* Molecular microbiology, 2013. **90**(1): p. 22-35.
17. Ene, I.V., et al., *Phenotypic Profiling Reveals that Candida albicans Opaque Cells Represent a Metabolically Specialized Cell State Compared to Default White Cells.* mBio, 2016. **7**(6): p. e01269-16.
18. Craik, V.B., A.D. Johnson, and M.B. Lohse, *Sensitivity of White and Opaque Candida albicans Cells to Antifungal Drugs.* Antimicrobial Agents and Chemotherapy, 2017. **61**(8): p. e00166-17.
19. Zhang, N., et al., *Selective Advantages of a Parasexual Cycle for the Yeast Candida albicans.* Genetics, 2015. **200**(4): p. 1117-1132.
20. Sasse, C., et al., *White-opaque switching of Candida albicans allows immune evasion in an environment-dependent fashion.* Eukaryotic cell, 2013. **12**(1): p. 50-58.

21. Sun, Y., et al., *pH Regulates White-Opaque Switching and Sexual Mating in Candida albicans.* Eukaryotic cell, 2015. **14**(11): p. 1127-1134.
22. Slutsky, B., J. Buffo, and D.R. Soll, *High-frequency switching of colony morphology in Candida albicans.* Science, 1985. **230**(4726): p. 666-9.
23. Kennedy, M.J., et al., *Variation in adhesion and cell surface hydrophobicity in Candida albicans white and opaque phenotypes.* Mycopathologia, 1988. **102**(3): p. 149-56.
24. Soll, D.R., S.R. Lockhart, and R. Zhao, *Relationship between switching and mating in Candida albicans.* Eukaryotic cell, 2003. **2**(3): p. 390-397.
25. Tao, L., et al., *Discovery of a "white-gray-opaque" tristable phenotypic switching system in candida albicans: roles of non-genetic diversity in host adaptation.* PLoS biology, 2014. **12**(4): p. e1001830-e1001830.
26. Bennett, R.J. and A.D. Johnson, *MATING IN CANDIDA ALBICANS AND THE SEARCH FOR A SEXUAL CYCLE.* Annual Review of Microbiology, 2005. **59**(1): p. 233-255.
27. Anderson, J., R. Mihalik, and D.R. Soll, *Ultrastructure and antigenicity of the unique cell wall pimple of the Candida opaque phenotype.* Journal of bacteriology, 1990. **172**(1): p. 224-235.
28. Kvaal, C., et al., *Misexpression of the opaque-phase-specific gene PEP1 (SAP1) in the white phase of Candida albicans confers increased virulence in a mouse model of cutaneous infection.* Infection and immunity, 1999. **67**(12): p. 6652-6662.
29. Lohse, M.B. and A.D. Johnson, *Temporal anatomy of an epigenetic switch in cell programming: the white-opaque transition of C. albicans.* Molecular microbiology, 2010. **78**(2): p. 331-343.
30. Pappas, P.G., *Invasive candidiasis.* Infect Dis Clin North Am, 2006. **20**(3): p. 485-506.
31. Takagi, J., et al., *Candida albicans white and opaque cells exhibit distinct spectra of organ colonization in mouse models of infection.* PloS one, 2019. **14**(6): p. e0218037-e0218037.
32. Anderson, J., et al., *Hypha formation in the white-opaque transition of Candida albicans.* Infection and immunity, 1989. **57**(2): p. 458-467.
33. Kolotila, M.P. and R.D. Diamond, *Effects of neutrophils and in vitro oxidants on survival and phenotypic switching of Candida albicans WO-1.* Infection and Immunity, 1990. **58**(5): p. 1174-1179.
34. Lohse, M.B. and A.D. Johnson, *Differential phagocytosis of white versus opaque Candida albicans by Drosophila and mouse phagocytes.* PloS one, 2008. **3**(1): p. e1473-e1473.
35. Bockmühl, D.P., et al., *Distinct and redundant roles of the two protein kinase A isoforms Tpk1p and Tpk2p in morphogenesis and growth of Candida albicans.* Molecular Microbiology, 2001. **42**(5): p. 1243-1257.
36. Huang, G., et al., *N-acetylglucosamine induces white to opaque switching, a mating prerequisite in Candida albicans.* PLoS pathogens, 2010. **6**(3): p. e1000806-e1000806.
37. Lan, C.-Y., et al., *Metabolic specialization associated with phenotypic switching in Candidaalbicans.* Proceedings of the National Academy of Sciences of the United States of America, 2002. **99**(23): p. 14907-14912.
38. Tsong, A.E., et al., *Evolution of a combinatorial transcriptional circuit: a case study in yeasts.* Cell, 2003. **115**(4): p. 389-99.
39. Calderone, R.A. and C.J. Clancy, *Candida and Candidiasis, Second Edition*. 2012: American Society of Microbiology.
40. Herskowitz, I., *A regulatory hierarchy for cell specialization in yeast.* Nature, 1989. **342**(6251): p. 749-57.
41. Yuen, K., et al., *Systematic genome instability screens in yeast and their potential relevance to cancer.* Proceedings of the National Academy of Sciences of the United States of America, 2007. **104**: p. 3925-30.

42. Haber, J.E., *Mating-type genes and MAT switching in Saccharomyces cerevisiae.* Genetics, 2012. **191**(1): p. 33-64.
43. Hull, C.M., R.M. Raisner, and A.D. Johnson, *Evidence for mating of the "asexual" yeast Candida albicans in a mammalian host.* Science, 2000. **289**(5477): p. 307-10.
44. Hull, C.M. and A.D. Johnson, *Identification of a mating type-like locus in the asexual pathogenic yeast Candida albicans.* Science, 1999. **285**(5431): p. 1271-5.
45. Magee, B.B. and P.T. Magee, *Induction of mating in Candida albicans by construction of MTLa and MTLalpha strains.* Science, 2000. **289**(5477): p. 310-3.
46. Bennett, R.J., *The parasexual lifestyle of Candida albicans.* Current opinion in microbiology, 2015. **28**: p. 10-17.
47. Lee, S.C., et al., *The Evolution of Sex: a Perspective from the Fungal Kingdom.* Microbiology and molecular biology reviews : MMBR, 2010. **74**: p. 298-340.
48. Pujol, C., et al., *The closely related species Candida albicans and Candida dubliniensis can mate.* Eukaryotic cell, 2004. **3**(4): p. 1015-1027.
49. Hickman, M.A., et al., *The 'obligate diploid' Candida albicans forms mating-competent haploids.* Nature, 2013. **494**(7435): p. 55-59.
50. Soll, D.R., *Mating-type locus homozygosis, phenotypic switching and mating: a unique sequence of dependencies in Candida albicans.* Bioessays, 2004. **26**(1): p. 10-20.
51. Zordan, R.E., et al., *Interlocking transcriptional feedback loops control white-opaque switching in Candida albicans.* PLoS biology, 2007. **5**(10): p. e256-e256.
52. Huang, G., et al., *Bistable expression of WOR1, a master regulator of white-opaque switching in Candida albicans.* Proceedings of the National Academy of Sciences of the United States of America, 2006. **103**(34): p. 12813-12818.
53. Huang, G., et al., *Bistable expression of WOR1, a master regulator of white–opaque switching in Candida albicans.* Proceedings of the National Academy of Sciences, 2006. **103**(34): p. 12813-12818.
54. Srikantha, T., et al., *TOS9 regulates white-opaque switching in Candida albicans.* Eukaryotic cell, 2006. **5**(10): p. 1674-1687.
55. Lockhart, S.R., et al., *In Candida albicans, white-opaque switchers are homozygous for mating type.* Genetics, 2002. **162**(2): p. 737-745.
56. Ramírez-Zavala, B., et al., *Environmental induction of white-opaque switching in Candida albicans.* PLoS pathogens, 2008. **4**(6): p. e1000089-e1000089.
57. Wang, J.M., R.J. Bennett, and M.Z. Anderson, *The Genome of the Human Pathogen Candida albicans Is Shaped by Mutation and Cryptic Sexual Recombination.* mBio, 2018. **9**(5): p. e01205-18.
58. Suwunnakorn, S., H. Wakabayashi, and E. Rustchenko, *Chromosome 5 of Human Pathogen Candida albicans Carries Multiple Genes for Negative Control of Caspofungin and Anidulafungin Susceptibility.* Antimicrobial agents and chemotherapy, 2016. **60**(12): p. 7457-7467.
59. Lohse, M.B. and A.D. Johnson, *Identification and Characterization of Wor4, a New Transcriptional Regulator of White-Opaque Switching.* G3 (Bethesda, Md.), 2016. **6**(3): p. 721-729.
60. Alkafeef, S.S., et al., *Wor1 establishes opaque cell fate through inhibition of the general co-repressor Tup1 in Candida albicans.* PLoS genetics, 2018. **14**(1): p. e1007176-e1007176.
61. Park, Y.-N., et al., *EFG1 Mutations, Phenotypic Switching, and Colonization by Clinical a/α Strains of Candida albicans.* mSphere, 2020. **5**(1): p. e00795-19.
62. Sun, Y., et al., *Deletion of a Yci1 Domain Protein of Candida albicans Allows Homothallic Mating in MTL Heterozygous Cells.* mBio, 2016. **7**(2): p. e00465.

63. Vyas, V., M. Barrasa, and G. Fink, *A CRISPR system permits genetic engineering of essential genes and gene families.* Science Advances, 2015. **1**.
64. Min, K., et al., *Candida albicans Gene Deletion with a Transient CRISPR-Cas9 System.* mSphere, 2016. **1**(3): p. e00130-16.
65. Noble, S.M. and A.D. Johnson, *Strains and strategies for large-scale gene deletion studies of the diploid human fungal pathogen Candida albicans.* Eukaryotic cell, 2005. **4**(2): p. 298-309.
66. Rothstein, R.J., *One-step gene disruption in yeast.* Methods Enzymol, 1983. **101**: p. 202-11.
67. Blackwell, C., et al., *Protein A-tagging for purification of native macromolecular complexes fromCandida albicans.* Yeast (Chichester, England), 2003. **20**: p. 1235-41.
68. Xie, J., et al., *N-acetylglucosamine induces white-to-opaque switching and mating in Candida tropicalis, providing new insights into adaptation and fungal sexual evolution.* Eukaryotic cell, 2012. **11**(6): p. 773-782.
69. Dignard, D. and M. Whiteway, *SST2, a regulator of G-protein signaling for the Candida albicans mating response pathway.* Eukaryotic cell, 2006. **5**(1): p. 192-202.
70. He, F., *Bradford Protein Assay.* Bio-protocol, 2011. **1**(6): p. e45.
71. Pal, S., et al., *Impaired cohesion and homologous recombination during replicative aging in budding yeast.* Science Advances, 2018. **4**(2): p. eaaq0236.
72. Li, Y., et al., *An intron with a constitutive transport element is retained in a Tap messenger RNA.* Nature, 2006. **443**(7108): p. 234-7.
73. Chen, Y., et al., *Chemogenomic Profiling of the Fungal Pathogen Candida albicans.* Antimicrobial agents and chemotherapy, 2018. **62**(2): p. e02365-17.
74. Tuch, B.B., et al., *The transcriptomes of two heritable cell types illuminate the circuit governing their differentiation.* PLoS genetics, 2010. **6**(8): p. e1001070-e1001070.
75. Sun, Y., *Analysis of Mating Circuitry in The Fungal Pathogen Candida albicans*, in *Biology*. 2016, Concordia University: unpuplished.
76. Xie, J., et al., *White-opaque switching in natural MTLa/α isolates of Candida albicans: evolutionary implications for roles in host adaptation, pathogenesis, and sex.* PLoS biology, 2013. **11**(3): p. e1001525-e1001525.
77. Scaduto, C., et al., *Epigenetic control of pheromone MAPK signaling determines sexual fecundity in Candida albicans.* Proceedings of the National Academy of Sciences, 2017. **114**: p. 201711141.
78. Srikantha, T., et al., *Nonsex genes in the mating type locus of Candida albicans play roles in a/α biofilm formation, including impermeability and fluconazole resistance.* PLoS pathogens, 2012. **8**(1): p. e1002476-e1002476.
79. Ahnesorg, P., P. Smith, and S.P. Jackson, *XLF interacts with the XRCC4-DNA ligase IV complex to promote DNA nonhomologous end-joining.* Cell, 2006. **124**(2): p. 301-13.
80. Daley, J.M., et al., *Nonhomologous end joining in yeast.* Annu Rev Genet, 2005. **39**: p. 431-51.
81. Soulard, A., et al., *The rapamycin-sensitive phosphoproteome reveals that TOR controls protein kinase A toward some but not all substrates.* Molecular biology of the cell, 2010. **21**(19): p. 3475-3486.
82. Swaney, D.L., et al., *Global analysis of phosphorylation and ubiquitylation cross-talk in protein degradation.* Nature methods, 2013. **10**(7): p. 676-682.
83. Altschul, S.F., et al., *Gapped BLAST and PSI-BLAST: a new generation of protein database search programs.* Nucleic acids research, 1997. **25**(17): p. 3389-3402.
84. Gonzalez-Rodriguez, Y. and S.F. Bunting, *XLF extends its range from DNA repair to replication.* The Journal of cell biology, 2019. **218**(7): p. 2075-2076.
85. Hickman, M.A., et al., *The 'obligate diploid' Candida albicans forms mating-competent haploids.* Nature, 2013. **494**(7435): p. 55-9.

86. Mahaney, B.L., et al., *XRCC4 and XLF form long helical protein filaments suitable for DNA end protection and alignment to facilitate DNA double strand break repair.* Biochemistry and cell biology = Biochimie et biologie cellulaire, 2013. **91**(1): p. 31-41.
87. Normanno, D., et al., *Mutational phospho-mimicry reveals a regulatory role for the XRCC4 and XLF C-terminal tails in modulating DNA bridging during classical non-homologous end joining.* eLife, 2017. **6**: p. e22900.
88. Bennett, R.J., et al., *Identification and characterization of a Candida albicans mating pheromone.* Molecular and cellular biology, 2003. **23**(22): p. 8189-8201.
89. Yi, S., et al., *The same receptor, G protein, and mitogen-activated protein kinase pathway activate different downstream regulators in the alternative white and opaque pheromone responses of Candida albicans.* Mol Biol Cell, 2008. **19**(3): p. 957-70.
90. Sahni, N., et al., *Tec1 mediates the pheromone response of the white phenotype of Candida albicans: insights into the evolution of new signal transduction pathways.* PLoS biology, 2010. **8**(5): p. e1000363-e1000363.
91. Soll, D.R., *Why does Candida albicans switch?* FEMS Yeast Research, 2009. **9**(7): p. 973-989.
92. Rastghalam, G., et al., *MAP Kinase Regulation of the Candida albicans Pheromone Pathway.* mSphere, 2019. **4**(1): p. e00598-18.
93. Saraste, M., P.R. Sibbald, and A. Wittinghofer, *The P-loop — a common motif in ATP- and GTP-binding proteins.* Trends in Biochemical Sciences, 1990. **15**(11): p. 430-434.
94. Kelley, L.A., et al., *The Phyre2 web portal for protein modeling, prediction and analysis.* Nature protocols, 2015. **10**(6): p. 845-858.
95. Whiteway, M. and C. Bachewich, *Morphogenesis in Candida albicans.* Annual Review of Microbiology, 2007. **61**(1): p. 529-553.
96. Zordan, R.E., D.J. Galgoczy, and A.D. Johnson, *Epigenetic properties of white-opaque switching in Candida albicans are based on a self-sustaining transcriptional feedback loop.* Proceedings of the National Academy of Sciences of the United States of America, 2006. **103**(34): p. 12807-12812.
97. Hull, C. and J. Heitman, *Fungal Mating: Candida albicans Flips a Switch to Get in the Mood.* Current biology : CB, 2002. **12**: p. R782-4.
98. Pendrak, M.L., S.S. Yan, and D.D. Roberts, *Hemoglobin Regulates Expression of an Activator of Mating-Type Locus α Genes in Candida albicans.* Eukaryotic Cell, 2004. **3**(3): p. 764-775.
99. Lachke, S.A., T. Srikantha, and D.R. Soll, *The regulation of EFG1 in white-opaque switching in Candida albicans involves overlapping promoters.* Mol Microbiol, 2003. **48**(2): p. 523-36.
100. Su, C., et al., *Hyphal induction under the condition without inoculation in Candida albicans is triggered by Brg1-mediated removal of NRG1 inhibition.* Mol Microbiol, 2018. **108**(4): p. 410-423.
101. Kadosh, D. and A.D. Johnson, *Rfg1, a protein related to the Saccharomyces cerevisiae hypoxic regulator Rox1, controls filamentous growth and virulence in Candida albicans.* Molecular and cellular biology, 2001. **21**(7): p. 2496-2505.
102. Park, Y.-N., et al., *Roles of the Transcription Factors Sfl2 and Efg1 in White-Opaque Switching in a/α Strains of Candida albicans.* mSphere, 2019. **4**(2): p. e00703-18.
103. Scaduto, C.M., et al., *Epigenetic control of pheromone MAPK signaling determines sexual fecundity in Candida albicans.* Proceedings of the National Academy of Sciences of the United States of America, 2017. **114**(52): p. 13780-13785.
104. Ene, I.V. and R.J. Bennett, *Hwp1 and related adhesins contribute to both mating and biofilm formation in Candida albicans.* Eukaryotic cell, 2009. **8**(12): p. 1909-1913.
105. Sharkey, L.L., et al., *HWP1 functions in the morphological development of Candida albicans downstream of EFG1, TUP1, and RBF1.* Journal of bacteriology, 1999. **181**(17): p. 5273-5279.

106. Braun, B.R. and A.D. Johnson, *TUP1, CPH1 and EFG1 make independent contributions to filamentation in candida albicans.* Genetics, 2000. **155**(1): p. 57-67.
107. Xu, H., et al., *S. oralis activates the Efg1 filamentation pathway in C. albicans to promote cross-kingdom interactions and mucosal biofilms.* Virulence, 2017. **8**(8): p. 1602-1617.
108. Dignard, D., et al., *Identification and characterization of MFA1, the gene encoding Candida albicans a-factor pheromone.* Eukaryotic cell, 2007. **6**(3): p. 487-494.
109. Yi, S., et al., *A Candida albicans-specific region of the alpha-pheromone receptor plays a selective role in the white cell pheromone response.* Mol Microbiol, 2009. **71**(4): p. 925-47.
110. Schaefer, D., et al., *Barrier activity in Candida albicans mediates pheromone degradation and promotes mating.* Eukaryotic cell, 2007. **6**(6): p. 907-918.
111. Panwar, S.L., et al., *MFalpha1, the gene encoding the alpha mating pheromone of Candida albicans.* Eukaryotic cell, 2003. **2**(6): p. 1350-1360.
112. Zhao, R., et al., *Unique aspects of gene expression during Candida albicans mating and possible G(1) dependency.* Eukaryotic cell, 2005. **4**(7): p. 1175-1190.
113. Bennett, R.J. and A.D. Johnson, *The role of nutrient regulation and the Gpa2 protein in the mating pheromone response of C. albicans.* Mol Microbiol, 2006. **62**(1): p. 100-19.
114. Singh, R.P., et al., *Cap2-HAP complex is a critical transcriptional regulator that has dual but contrasting roles in regulation of iron homeostasis in Candida albicans.* The Journal of biological chemistry, 2011. **286**(28): p. 25154-25170.
115. Bahn, Y.-S., et al., *Genome-wide transcriptional profiling of the cyclic AMP-dependent signaling pathway during morphogenic transitions of Candida albicans.* Eukaryotic cell, 2007. **6**(12): p. 2376-2390.
116. Fernández-Arenas, E., et al., *Integrated proteomics and genomics strategies bring new insight into Candida albicans response upon macrophage interaction.* Mol Cell Proteomics, 2007. **6**(3): p. 460-78.
117. De Groot, P.W., K.J. Hellingwerf, and F.M. Klis, *Genome-wide identification of fungal GPI proteins.* Yeast, 2003. **20**(9): p. 781-96.
118. Urban, C., et al., *Identification of cell surface determinants in Candida albicans reveals Tsa1p, a protein differentially localized in the cell.* FEBS Lett, 2003. **544**(1-3): p. 228-35.
119. Hernday, A.D., et al., *Ssn6 Defines a New Level of Regulation of White-Opaque Switching in Candida albicans and Is Required For the Stochasticity of the Switch.* mBio, 2016. **7**(1): p. e01565.
120. Lohse, M.B., et al., *Identification and characterization of a previously undescribed family of sequence-specific DNA-binding domains.* Proceedings of the National Academy of Sciences of the United States of America, 2013. **110**(19): p. 7660-7665.
121. Mignone, F., et al., *Untranslated regions of mRNAs.* Genome biology, 2002. **3**(3): p. REVIEWS0004-REVIEWS0004.
122. Tomari, Y. and P.D. Zamore, *Perspective: machines for RNAi.* Genes Dev, 2005. **19**(5): p. 517-29.
123. Malone, C.D. and G.J. Hannon, *Small RNAs as guardians of the genome.* Cell, 2009. **136**(4): p. 656-668.
124. Bernstein, D.A., et al., *Candida albicans Dicer (CaDcr1) is required for efficient ribosomal and spliceosomal RNA maturation.* Proceedings of the National Academy of Sciences, 2012. **109**(2): p. 523-528.
125. Kaneva, I.N., et al., *Proteins that physically interact with the phosphatase Cdc14 in Candida albicans have diverse roles in the cell cycle.* Scientific reports, 2019. **9**(1): p. 6258-6258.
126. Altschul, S.F., et al., *Protein database searches using compositionally adjusted substitution matrices.* Febs j, 2005. **272**(20): p. 5101-9.
127. Lin, C.-H., et al., *Genetic control of conventional and pheromone-stimulated biofilm formation in Candida albicans.* PLoS pathogens, 2013. **9**(4): p. e1003305-e1003305.

Name	Description	Sequence (5′ to 3′)	Source
ORF3-del-for	*ORF19.7060* deletion PCR cassette forward primer	TGGAGTTGCAAACGACCAAGTACCATAAATCCATA TGGTTTCCAGTTAGAGTTGATAATTAGCATAGTCAA TTCTTTTgaagcttcgtacgctgcaggtc	This study
ORF19.7060-del-Rev	*ORF19.7060* deletion PCR cassette reverse primer	TGATAGCTCGTTGGAATAAAATGGCAGATACTGTAT AGTAAGTTTATAAATCTCAAGTAAGTTACAATTTTC GTATATctgatatcatcgatgaattcgag	This study
ORF19.7060-sg-up	*ORF19.7060* guide DNA forward	atttgTGTTCCGACTTCAATGTCTCg	This study
ORF19.7060-sg-down	*ORF19.7060* guide DNA reverse	aaaacGAGACATTGAAGTCGGAACAc	This study
ORF19.7060-ex-for	*ORF19.7060* external forward primer	ATGGTTTCCAGTTAGAGTTG	This study
ORF19.7060-ex-Rev	*ORF19.7060* external reverse primer	TTGAAATGGTTGATAGCTCG	This study

*MTL***a***1*-F	*MTL***a***1* forward primer	TTGAAGCGTGAGAGGCAGGAG	Magee
*MTL***a***1*-R	*MTLa1* reverse primer	GTTTGGGTTCCTTCTTTCTCATTC	Magee
MTLα2-F	*MTLα2* forward primer	TTCGAGTACATTCTGGTCGC	Magee
MTLα2-R	*MTLα2* reverse primer	TGTAAACATCCTCAATTGTACCCG	Magee
ORF19.7060-pro-del-for1	*ORF19.7060* promoter deletion PCR cassette forward primer1	AGTTCATCCTTTTTTTTTCCTTCCCTCCAACGTCATGTTGTAGAATTAAACATAATGGTGCATCAAATTACATATAgaagcttcgtacgctgcaggtc	This study
ORF19.7060-pro-del-for2	*ORF19.7060* promoter deletion PCR cassette forward primer2	CTTCTAATGAAATTCCTCAATTGTGTGACAGAGTGCACAAGGACTACCTATCAAAAAGAAAATCAGATTCTCAACCTgaagcttcgtacgctgcaggtc	This study

ORF19.7060-pro-del-for3	*ORF19.7060* promoter deletion PCR cassette forward primer3	AGATATTTGATATCACTTGCAGGCGTTCCCGGCTCTGGTAAAACAACATTTGCTAATGCTATAGCCAAAAGACTTTCgaagcttcgtacgctgcaggtc	This study
ORF19.7060-pro-del-for4	*ORF19.7060* promoter deletion PCR cassette forward primer4	AACTTTTGCAAAAGTGGTAGTACTATCTCAAGATGGGTTTCATTTATATCGCTCGGAACTAACATTAATGGCAGATCgaagcttcgtacgctgcaggtc	This study
ORF19.7060-pro-del-for5	*ORF19.7060* promoter deletion PCR cassette forward primer5	CAAAGGAGGCTTTTCGAAGACGGGGTGCTCCTTTTACTTTTAACGCACAGGCTTTTGTCAATTTGATCTCAAAATTGgaagcttcgtacgctgcaggtc	This study
ORF19.7060-pro-del-for6	*ORF19.7060* promoter deletion PCR cassette forward primer6	AAGGACCGTTCCCAAACCATCAAAGCACCTTCTTTTGATCACAAATTGAAAGATCCGATAGAAGATGATATAGTGATgaagcttcgtacgctgcaggtc	This study
ORF19.7060-pro-del-for7	*ORF19.7060* promoter deletion PCR cassette forward primer7	ACACGGTAATGTAGACATTATAATAATCGAAGGAAATTATGTATCACTTCGAGACAAATACTGGGATGAAATTGAAAgaagcttcgtacgctgcaggtc	This study

ORF19.7060-pro-del-for8	*ORF19.7060* promoter deletion PCR cassette forward primer8	ATTTTGTTGACGACACTTGGTTTATAAAAACCCCTGAAAATCTAGTTCGAGAGAGAATTATTAAACGCCATTTGAACgaagcttcgtacgctgcaggtc	This study
ORF19.7060-pro-del-Rev	*ORF19.7060* promoter deletion PCR cassette reverse primer8	ATACCTTTTGTATTGAAATATTTGGATAGTGAGTTGTCGGCAATGGGTATAAAGATGCGTTATAATGTTGAACCAActgatatcatcgatgaattcgag	This study
ORF19.7060-pro-ex-for	*ORF19.7060* promoter external forward primer	GGACTTGGCTATCCATTGTG	This study
ORF19.7060-pro-ex-Rev	*ORF19.7060* promoter external reverse primer	GAGCCAATGTACTCTGGTGC	This study
ORF19.7060-pro-del-for	*ORF19.7060* promoter deletion PCR cassette forward primer	CCATATATACAAGGTTTTTCTTGCCCTAGAAATGGTATGGACTTGGCTATCCATTGTGTTGGGAAAAGTGACATCACgaagcttcgtacgctgcaggtc	This study

ORF19.7060-pro-del-rev	*ORF19.7060* promoter deletion PCR cassette reverse primer	ATACCTTTTGTATTGAAATATTTGGATAGTGAGTTGTCGGCAATGGGTATAAAGATGCGTTATAATGTTGAACCAActgatatcatcgatgaattcgag	This study
ORF19.7060-pro-sg-up	*ORF19.7060* promoter guide DNA forward	atttgAAGAAAAAAGAAAATTATGCg	This study
ORF19.7060-pro-sg-down	*ORF19.7060* promoter guide DNA reverse	aaaacGCATAATTTTCTTTTTTCTTc	This study
HIS1-F	*HIS1* forward primer	TTTAGTCAATCATTTACCAGACCG	This study
HIS1-R	*HIS1* reverse primer	TCTATGGCCTTTAACCCAGCTG	This study
ORF19.7060-pro-ex-for	*ORF19.7060* promoter external forward primer	GGACTTGGCTATCCATTGTG	This study
ORF19.7060-pro-ex-Rev	*ORF19.7060* promoter external reverse primer	GAGCCAATGTACTCTGGTGC	This study

Table S1. The primers are used in this study